AD-A070 442 ARNOLD ENGINEERING DEVELOPMENT CENTER ARNOLD AFS TN F/G 22/2
DATA VERIFICATION TESTS OF A 0.03-SCALE NASA SPACE SHUTTLE LAUN--ETC(U)
NOV 78 J A BLACK, R E GRAHAM
UNCLASSIFIED AEDC-TSR-78-P54 NL

1 OF 1
AD
A070442

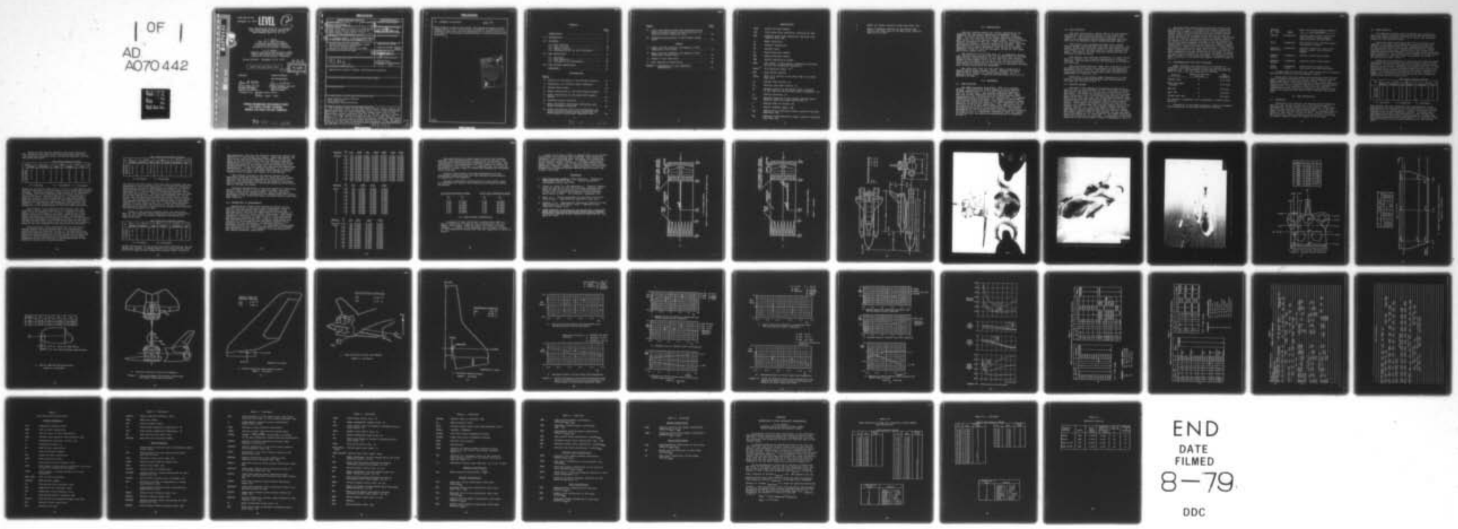

END
DATE
FILMED
8-79
DDC

AEDC-TSR-78-P54

November 27, 1978

LEVEL

DATA VERIFICATION TESTS OF A 0.03-SCALE NASA SPACE SHUTTLE LAUNCH VEHICLE AT MACH NUMBERS FROM 0.60 TO 1.55

J. A. Black
ARO, Inc., AEDC Division
A Sverdrup Corporation Company
Propulsion Wind Tunnel Facility
Arnold Air Force Station, Tennessee

R. E. Graham
Analysis and Evaluation Division (DOTA)
Arnold Engineering Development Center
Arnold Air Force Station, Tennessee

Period Covered: September 19-20, 1978

Approved for public release; distribution unlimited.

Reviewed By:

JAMES M. McGEE, 1st Lt, USAF
Test Director, PWT Division
Directorate of Test Operations

Approved for Publication:

FOR THE COMMANDER

JAMES D. SANDERS, Colonel, USAF
Director of Test Operations
Deputy for Operations

Prepared for: Johnson Space Center
EX 33
Houston, Texas 77058

ARNOLD ENGINEERING DEVELOPMENT CENTER
AIR FORCE SYSTEMS COMMAND
ARNOLD AIR FORCE STATION, TENNESSEE

UNCLASSIFIED

REPORT DOCUMENTATION PAGE		READ INSTRUCTIONS BEFORE COMPLETING FORM
1. REPORT NUMBER (14) AEDC-TSR-78-P54	2. GOVT ACCESSION NO.	3. RECIPIENT'S CATALOG NUMBER (9)
4. TITLE (and Subtitle) (6) Data Verification Tests of a 0.03-Scale NASA Space Shuttle Launch Vehicle at Mach Numbers from 0.60 to 1.55.		5. TYPE OF REPORT & PERIOD COVERED Final Report, Sept. 20-30, 1978
		6. PERFORMING ORG. REPORT NUMBER
7. AUTHOR(s) (10) J. A. Black and R. E. Graham, ARO, Inc., a Sverdrup Corporation Company		8. CONTRACT OR GRANT NUMBER(s)
9. PERFORMING ORGANIZATION NAME AND ADDRESS Arnold Engineering Development Center Air Force Systems Command Arnold Air Force Station, TN 37389		10. PROGRAM ELEMENT, PROJECT, TASK AREA & WORK UNIT NUMBERS Program Element 921E01 65807F
11. CONTROLLING OFFICE NAME AND ADDRESS 042 550		12. REPORT DATE (11) November 1978
		13. NUMBER OF PAGES 48
14. MONITORING AGENCY NAME & ADDRESS(if different from Controlling Office) (12) 51 p.		15. SECURITY CLASS. (of this report) Unclassified
		15a. DECLASSIFICATION/DOWNGRADING SCHEDULE N/A

16. DISTRIBUTION STATEMENT (of this Report)

Approved for public release; distribution unlimited.

17. DISTRIBUTION STATEMENT (of the abstract entered in Block 20, if different from Report)

18. SUPPLEMENTARY NOTES

19. KEY WORDS (Continue on reverse side if necessary and identify by block number)

Space Shuttle Launch Vehicle
Flow angularity
Aerodynamic characteristics

20. ABSTRACT (Continue on reverse side if necessary and identify by block number)

A 0.03-scale model of the NASA Space Shuttle Launch Vehicle was tested September 19-20 and September 29-30, 1978, in the Propulsion Wind Tunnel (16T) at free-stream Mach numbers from 0.60 to 1.55, free-stream dynamic pressures from 387 to 658 psf, angles of attack from -8 to 8 deg, angles of sideslip from -6 to 6 deg, and roll angles of 0, 180, 90, and -90 deg with nominal inboard elevon deflections of 10 deg and outboard elevon deflections of 5 deg. The objectives of the test were to determine flow angularity on the standard → over

DD FORM 1 JAN 73 1473 EDITION OF 1 NOV 65 IS OBSOLETE 042 550

UNCLASSIFIED

20. ABSTRACT (Concluded)

alpha/beta

sting support system (first entry) and high-pitch support system (second entry), and to provide data throughout an α/β matrix to establish a data base for the determination of angular corrections to be applied to previously obtained data if such corrections are necessary.

Accession For	
NTIS GRA&I	✓
DDC TAB	
Unannounced	
Justification	
By	
Distribution/	
Availability Codes	
Dist	Avail and/or special
A	

AFSC
Arnold AFS Tenn

CONTENTS

ILLUSTRATIONS

TABLES

NOMENCLATURE

AADS	Ascent Air Data System
AFA	Pitch plane flow angularity, positive up, deg
BFA	Sideslip plane flow angularity, positive from right to left, deg
$\mathcal{C}_L$	Model centerline
CP	Pressure coefficient
ET	External tank
M_∞	Free-stream Mach number
MRC	Moment reference center
OMS	Orbital maneuvering system
PART	Part number (a data subset containing variations of only one independent parameter)
$Rex10^{-6}$	Unit Reynolds number, ft^{-1}
SRB	Solid rocket booster
X/C_{BF}	Ratio of a station on the body flap to the body flap chord
X_O	Orbiter body station, in.
X_T	External tank body station, in.
Y_O	Lateral station on the orbiter base, positive to the right of the vertical plane of symmetry, in.
Z_O	Orbiter waterline, in.
Z_{orb}	Vertical location of the orbiter balance center, positive above the tunnel centerline, ft
α	Orbiter angle of attack, deg
β	Orbiter sideslip angle, deg
δ_{e_I}	Inboard elevon deflection angle, positive trailing edge down, deg
δ_{e_O}	Outboard elevon deflection angle, positive trailing edge down, deg

ϕ	Model roll angle, positive right wing down, deg
η	Ratio of spanwise station on the orbiter body flap to the total span of the body flap, positive from left to right

1.0 INTRODUCTION

The work reported herein was jointly sponsored by and conducted for the Arnold Engineering Development Center (AEDC)/DO and the Johnson Space Center, NASA/JSC, Houston, Texas. The work was done at the Arnold Engineering Development Center, Air Force Systems Command (AFSC), Arnold Air Force Station, Tennessee by ARO, Inc., AEDC Division (a Sverdrup Corporation Company), contract operator of the AEDC. The test was conducted in the Propulsion Wind Tunnel Facility (PWT), Propulsion Wind Tunnel, Transonic (16T) during the periods September 19 and 20, 1978 and September 29 and 30, 1978 under ARO Project Number P41T-35.

The objectives of the test were (1) to adequately define test section flow angularity for a 0.03-scale model of the NASA Space Shuttle Launch Vehicle in both the pitch and sideslip planes at Mach numbers from 0.60 to 1.55, and (2) to provide a data base throughout an α/β matrix for the determination of flow angularity corrections to be applied to previously obtained data if such corrections are necessary.

The final data from the test have been transmitted to Johnson Space Center, Houston, Texas. Requests for these data should be directed to Johnson Space Center, EX 33, Houston, Texas 77058. A copy of the final data is on file on microfilm at AEDC.

2.0 APPARATUS

2.1 TEST FACILITY

The AEDC Propulsion Wind Tunnel (16T) is a variable density, continuous-flow tunnel capable of being operated at Mach numbers from 0.2 to 1.6 and stagnation pressures from 120 to 4000 psfa. The maximum attainable Mach number can vary slightly depending upon the tunnel pressure ratio requirements with a particular test installation. The maximum stagnation pressure attainable is a function of Mach number and available electrical power. The tunnel stagnation temperature can be varied from about 80 to 160°F depending upon the available cooling water temperature. The test section is 16 ft square by 40 ft long and is enclosed by 60-deg inclined-hole perforated walls of six-percent porosity. The general arrangement of the test section with the test article installed is shown in Fig. 1. Additional information about the tunnel, its capabilities and operating characteristics is presented in Ref. 1.

2.2 TEST ARTICLES

The test article was a scaled replica of the Rockwell International Space Shuttle Vehicle in its launch configuration. The launch configuration consisted of the orbiter, an expendable external oxygen/hydrogen fuel tank (ET), and two expendable Solid Rocket Boosters (SRB's).

The orbiter has a blended wing body with a double delta planform (81 deg/45 deg) with full span elevons. The single, 45-deg swept vertical stabilizer had rudder deflection capability but was maintained at 0 deg throughout the tests. The single, aft body flap was present but was not deflected during the tests.

The external fuel tank was cylindrical in cross section having a tangent ogive forebody terminating in a biconic nose cap. The aft end of the ET was basically an ellipsoid of revolution.

The Solid Rocket Boosters (SRB) were attached to the ET by forward and aft attach lugs and were in the centerline horizontal plane of the ET. The SRB's were cylindrical in cross section and had an 18-deg semi-angle forebody which terminated in a spherical tip.

Dimensions of the primary model components are given in Fig. 2 and more detailed descriptions and drawings of the model may be found in Ref. 2.

2.3 SUPPORT SYSTEMS

The Tunnel 16T standard sting support system which is shown in Fig. 1a and described in Ref. 1 was used to support and position the model in the test section during the first test entry. The model was supported by a dual sting arrangement consisting of two 2.0-in.-diam stings exiting from the bases of the left and right hand solid rocket boosters (SRB). These stings were then attached by adapters to 4.16-in.-diam parallel stings which were mounted into the sting support system. This support arrangement allowed the base of the orbiter to be essentially free from any support system interference (see Fig. 3). The sting support system utilizes computer control to position the model at angles of attack and sideslip through combinations of pitch and roll angles. This model support system is advantangeous in that the model can be maintained at, or very close to, the tunnel centerline where flow angularity is a minimum. A photograph of the model installed on the sting support system is presented in Fig. 4.

The High-Pitch model support system was utilized for the second test entry. The High-Pitch support system was mounted into a dummy roll mechanism of the standard sting support system and utilized the vertical traverse feature of the latter system to maintain the orbiter as close to tunnel centerline as possible within the physical constraints of ±36 in. vertical traverse of the sting support system. The geometry of the High-Pitch support and the location of the orbiter model component relative to the supporting dual stings enabled the orbiter to be maintained close to tunnel centerline at angles of attack of zero deg or greater during pitch polars conducted at zero deg roll angle. During pitch polars conducted with the model roll 180 deg, the orbiter model component was below centerline at all angles of attack and its location relative to the tunnel centerline diverged as model angle of attack was increased. A photograph of the model installed on the High-Pitch support system is shown in Fig. 5.

2.4 INSTRUMENTATION AND TEST PROCEDURES

Model pressures were measured at 25 locations by individual transducers located inside the orbiter and the external tank. The locations of the pressure orifices are shown in Fig. 6 and are summarized as follows:

Location	Number of Pressure Orifices	Size Transducer
Orbiter base	9	±2.5 psid
Body Flap Upper Surface	8	±2.5 psid
OMS Pod	2	±10 psid
AADS (ET)	2	±10 psid
40-deg Cone (ET)	4	±10 psid

All pressure transducers were referenced to tunnel plenum pressure.

In addition to the model pressures, forces and moments were measured by strain-gage balances as follows:

Balance Location	Type	Model Forces and Moments Measured or Calculated
Orbiter	6-component	Orbiter normal force, side force, axial force, pitching-moment, rolling moment, yawing moment
Wing	3-component	Wing normal force, bending moment, and torsional moment
Vertical Stabilizer	3-component	Vertical stabilizer side force, bending moment, and torsional moment
Inboard Elevon	1-component	Inboard elevon hinge moment
Outboard Elevon	1-component	Outboard elevon hinge moment
*Dual Stings	4-component (each)	Launch vehicle normal force, side force, and pitching moment

*Primary use of data from the gaged stings was to calculate deflections resulting from aerodynamic loading.

Sting pitch and roll angles were determined from the outputs of synchro-transmitters during tests conducted with the model supported on the sting support system. During the second test entry, sting pitch and roll angles were determined from the outputs of a synchro-transmitter and a potentiometer, respectively. The electrical signals from all position indicating devices, strain-gage balances, and pressure transducers were digitized for on-line data reduction and tabulation.

3.0 TEST DESCRIPTION

3.1 PROCEDURE

During both test entries, the desired tunnel conditions were set and, during the portion of the tests devoted to determination of test section flow angularities, model angle of attack was varied at zero sideslip angle (ϕ = 0 and 180 deg), or model sideslip angle was varied at a nominal angle of attack of zero deg (ϕ = 90 and -90 deg). During testing of the α/β matrix, orbiter sideslip was varied from -6 to 6 deg at nominal constant angles of attack of -8 to 8 deg.

3.2 DATA REDUCTION

All measured pressures were converted into coefficient form, and those located on the base of the orbiter were used to correct measured normal force, axial force, and pitching moment for base pressure force.

Force and moment coefficient data for the orbiter were computed in the body axis coordinate system using the projection of the orbiter nose on the longitudinal centerline of the external tank as the moment reference point. Forces and moments from the wing, vertical tail, and elevons were computed about moment reference points unique to the individual model components. The locations of the moment reference points and directions of positive forces and moments are shown in the sketches of Figs. 2 and 7.

Values of flow angularity in the pitch and sideslip planes determined during the first test entry (sting support system) along with the vertical location of the orbiter balance center relative to the tunnel centerline are presented in Fig. 8. The data presented in Fig. 8a represent selected pitch plane flow angularity values determined from various model component balances. The listing below identifies the balance outputs considered in the determination of pitch plane flow angularity (AFA) during the first test entry.

AFA (Sting Support System)

M_∞	ϕ = 0,180			ϕ = -90,90		
	CNORB	CNSTING	CNW	CYORB	CYSTING	CSV
0.60	U	U	D	C	C	C
0.90	U	U	D	C	C	C
0.95	U	U	D	-	-	-
1.10	U	U	D	C	C	C
1.25	U	U	D	C	C	C
1.55	U	U	D	-	-	-

U = Utilized C = Considered D = Discarded

Wing balance data were discarded from consideration in the determination of AFA because of large zero shifts in that balance early in the testing period. Figure 8b presents various average values of AFA grouped as follows: all usable data (excepting wing data), data obtained at 0- and 180-deg roll, data obtained at ±90-deg roll, and depicted as a dashed line, the values selected by the investigator as the data correction, relying primarily on the values obtained at 0- and 180-deg roll.

Values of test section sideslip plane flow angularity, BFA, determined from the various balances during the first test entry are presented in Fig. 8c and the balances utilized are identified below:

BFA (Sting Support System)

M_∞	← ϕ = -90, 90		→ ← ϕ = 0,180 →		
	CNORB	CNSTING	CNW	CYORB	CSV
0.60	C	C	C	U	U
0.90	C	C	C	U	U
0.95	-	-	-	U	U
1.10	C	-	C	U	U
1.25	C	C	C	D	D
1.55	-	-	-	U	U

U = Utilized C = Considered D = Discarded

Except for the orbiter data at M_∞ = 1.55, ϕ = 0-and 180-deg roll, all data indicated a flow from right to left when viewed looking upstream. Figure 8d presents average values of BFA determined at 180-deg roll angle increments and the values selected as angle corrections. Values of BFA at M_∞ = 1.25 exhibited a departure from the trend established at other Mach numbers which is believed to be a result of some unknown flow field phenomena not necessarily associated with test section flow angularity. These values were therefore excluded from consideration in the determination of the flow field correction.

The location of the orbiter balance center (Fig. 8e) indicates a fairly small departure, as a function of pitch angle, from its location at α = 0 deg. Although the sting support system will normally maintain a model close to the tunnel centerline as sting pitch is varied, this desirable feature was precluded by two geometric factors; (1) the orbiter balance was positioned (at zero deg roll) above the horizontal plane of the sting system, and (2) the sting pitch requirements of the test required a pitch center aft of the model.

Flow angularity values determined for the 0.03-scale launch vehicle during the second test entry (high-pitch support system) are presented in Fig. 9. As with the first test entry presentation, Fig. 9a depicts the pitch plane flow angularity values determined from the various force measuring devices at 180-deg opposed roll orientations and the model component balance data utilized in the determination of the correction function are identified below.

AFA (High-Pitch Support System)

M_∞	ϕ = 0,180				ϕ = -90,90		
	CNORB	CNSTING	CNW	CBW	CYORB	CYSTING	CSV
0.60	D	U	D	U	U	U	U
0.90	D	U	D	U	U	U	U
1.10	D	D	D	-	-	-	-
1.25	D	D	D	U	U	U	U
1.55	D	U	D	U	-	-	-

U = Utilized D = Discarded

All orbiter and wing normal force data were discarded from consideration as were sting data at M_∞ = 1.10 and 1.25 because of non-parallel, non-linear characteristics exhibited at 180-deg roll orientation only. Wing bending was however given consideration at 0- and 180-deg roll orientation because the two data sets were parallel. Side force measurements were utilized at all Mach numbers at which tests were conducted at -90 and 90-deg roll and therefore provided the primary source of AFA values. The average values of all data as well as the 180-deg roll opposed measurements and the selected angle corrections (dashed line) are shown in Fig. 9b. A third order polynomial function of Mach number was utilized to fit the correction although any lower order function would probably have described the correction equally as well.

Values of test section sideslip plane flow angularity, BFA, for the high-pitch model supported tests are presented in Figs. 9c and d and the balance components considered are identified below.

BFA (High-Pitch Support System)

M_∞	ϕ = -90,90			ϕ = 0,180		
	CNORB	CNSTING	CNW	CYORB	CYSTING	CSV
0.60	D	D	D	U	U	U
0.90	D	D	D	U	U	U
1.10	-	-	-	U	U	U
1.25	D	D	D	U	U	U
1.55	-	-	-	U	U	U

U = Utilized D = Discarded

During the analysis of the normal force data obtained at -90 and 90-deg roll angles, it became evident that values of BFA determined from these balance components produced higher values of flow angularity than did the sideforce indicating balance components at 0- and 180-deg roll angles. Since the orbiter and the orbiter wing were effectively shielded at -90 deg roll angle by the ET and the SRB's from any crossflow component approaching from right to left, it was concluded that values of BFA determined by the orbiter and wing balances were not representative of the flow angularity and were eliminated from consideration. Values of BFA were therefore, as in the case of the first entry data, determined from sideforce balance component data at model roll angles of 0 and 180 deg.

The vertical location of the orbiter balance as the high-pitch sting was pitched, Fig. 9e, shows the large excursion from the centerline experienced by the balance at ϕ = 180 deg. The resultant proximity of the model to the tunnel floor could have produced the erroneous appearing normal-force data at 180-deg roll angle.

Following determination of the flow angularity corrections shown in Figs. 8b and d (sting support system), and Figs. 9b and d (high-pitch support system), the flow angularity correction functions indicated by the dashed lines were vectorally added to the uncorrected model attitudes during a post test data reduction.

3.3 UNCERTAINTY OF MEASUREMENTS

Uncertainties (bands which include 95 percent of the calibration data) of the basic tunnel parameters, shown in Fig. 10, were estimated from repeat calibrations of the instrumentation and from the repeatability and uniformity of the test section flow during tunnel calibration. Additional information concerning the uncertainties in the free-stream properties is discussed in Refs. 3 and 4. Uncertainties in the instrumentation systems were estimated from repeat calibrations of the systems against secondary standards whose uncertainties are traceable to the National Bureau of Standards calibration equipment. The instrument uncertainties are combined using the Taylor series method of error propagation described in Ref. 5 to determine the uncertainties of the reduced parameters shown below:

Balance	M_∞	α/β	ΔCNF	ΔCY	ΔCAF	ΔCMF	ΔCLL	ΔCLN
Orbiter	0.60	-4/0	±0.0048	±0.0041	±0.0018	±0.0033	±0.0005	±0.0027
	↓	4/0	±0.0049	±0.0041	±0.0017	±0.0033	±0.0005	±0.0027
	0.90	-4/0	±0.0035	±0.0031	±0.0012	±0.0024	±0.0003	±0.0020
	↓	4/0	±0.0036	±0.0031	±0.0012	±0.0024	±0.0003	±0.0020
	0.95	-4/0	±0.0034	±0.0029	±0.0011	±0.0023	±0.0003	±0.0020
	↓	4/0	±0.0034	±0.0029	±0.0011	±0.0023	±0.0003	±0.0020
	1.10	-4/0	±0.0031	±0.0027	±0.0010	±0.0021	±0.0003	±0.0018
	↓	4/0	±0.0032	±0.0027	±0.0010	±0.0022	±0.0003	±0.0018
	1.15	-4/0	±0.0031	±0.0027	±0.0010	±0.0021	±0.0003	±0.0018
	↓	4/0	±0.0031	±0.0027	±0.0010	±0.0021	±0.0003	±0.0018
	1.25	-4/0	±0.0030	±0.0026	±0.0009	±0.0020	±0.0003	±0.0017
	↓	4/0	±0.0030	±0.0026	±0.0009	±0.0020	±0.0003	±0.0017
	1.55	-4/0	±0.0028	±0.0024	±0.0009	±0.0019	±0.0003	±0.0016
↓	↓	4/0	±0.0028	±0.0024	±0.0009	±0.0019	±0.0003	±0.0016

Balance	M_∞	α/β	ΔCNW	ΔCTW	ΔCBW
Wing	0.60	-4/0	±0.0073	±0.0006	±0.0006
	↓	4/0	±0.0073	±0.0006	±0.0006
	0.90	-4/0	±0.0054	±0.0005	±0.0005
	↓	4/0	±0.0054	±0.0005	±0.0005
	0.95	-4/0	±0.0052	±0.0005	±0.0004
	↓	4/0	±0.0052	±0.0005	±0.0004
	1.10	-4/0	±0.0048	±0.0004	±0.0004
	↓	4/0	±0.0048	±0.0004	±0.0004
	1.15	-4/0	±0.0047	±0.0004	±0.0004
	↓	4/0	±0.0047	±0.0004	±0.0004
	1.25	-4/0	±0.0046	±0.0004	±0.0004
	↓	4/0	±0.0046	±0.0004	±0.0004
	1.55	-4/0	±0.0043	±0.0004	±0.0004
↓	↓	4/0	±0.0043	±0.0004	±0.0004

Balance	M_∞	α/β	ΔCSV	ΔCBV	ΔCTV
Vertical	0.60	-4/0	±0.0024	±0.0028	±0.0023
Tail	↓	4/0	±0.0024	±0.0028	±0.0023
	0.90	-4/0	±0.0018	±0.0021	±0.0017
	↓	4/0	±0.0018	±0.0021	±0.0017
	0.95	-4/0	±0.0017	±0.0020	±0.0017
	↓	4/0	±0.0017	±0.0020	±0.0017
	1.10	-4/0	±0.0016	±0.0018	±0.0015
	↓	4/0	±0.0016	±0.0018	±0.0015
	1.15	-4/0	±0.0016	±0.0018	±0.0015
	↓	4/0	±0.0016	±0.0018	±0.0015
	1.25	-4/0	±0.0015	±0.0017	±0.0015
	↓	4/0	±0.0015	±0.0017	±0.0015
	1.55	-4/0	±0.0014	±0.0016	±0.0014
↓	↓	4/0	±0.0014	±0.0016	±0.0014

The uncertainties in model angle of attack and sideslip resulting from uncertainties in sting pitch, sting roll, and sting/balance deflections were estimated to be ±0.10 deg. The uncertainty in the determination of flow angularity correction was estimated to be ±0.10 deg. In combined form, the final uncertainties in model angle of attack and sideslip are estimated to be ±0.14 deg.

Another, statistically oriented determination of the uncertainty associated with the flow angularity measurements is presented in the Appendix.

Pressure coefficient uncertainties for both model tests are estimated for typical test conditions and model attitudes as follows:

±2.5 psid Transducer Range		±10.0 psid Transducer Range	
M_∞	CP	M_∞	CP
0.60	±0.0074	0.60	±0.0096
0.90	±0.0041	0.90	±0.0071
0.95	±0.0038	0.95	±0.0068
1.10	±0.0033	1.10	±0.0062
1.15	±0.0031	1.15	±0.0061
1.25	±0.0029	1.25	±0.0059
1.55	±0.0024	1.55	±0.0056

4.0 DATA PACKAGE PRESENTATION

A summary of test conditions is presented in Tables 1 and 2 correlating the type of data acquired with test Part Number, Mach number, Reynolds number, and model attitude schedule. A sample of the tabulated data is shown in Table 3. The nomenclature associated with the tabulation is given in Table 4.

A copy of all data, either in tabular form or as a microfilm record, and including both corrected (flow angularity included), and uncorrected model attitudes, was transmitted to the following organizations: (1) Rockwell International Space Division, Downey, California, (2) NASA-Johnson Space Center, Houston, Texas, and (3) Marshall Space Flight Center, Huntsville, Alabama. Magnetic tapes containing all data were transmitted to Chrysler Michoud Defense Space Division, New Orleans, Louisiana.

REFERENCES

1. Test Facilities Handbook (Tenth Edition). "Propulsion Wind Tunnel Facility, Vol. 4." Arnold Engineering Development Center, May 1974.

2. Allen, E., Chee, E., and Hawthorne, P. "Pretest Information for Test IA-105A of the 0.03-Scale Pressure Loads Model 47-OTS of the Space Shuttle Integrated Vehicle in the 16-ft Transonic Test Section of the Propulsion Wind Tunnel at AEDC." SD 77-SH-0194, September 1977.

3. Gunn, J. A. "Check Calibration of the AEDC 16-ft Transonic Tunnel." AEDC-TR-66-80 (AD633277), May 1966.

4. Jackson, F. M. "Supplemental Calibration Results for the AEDC Propulsion Wind Tunnel (16T)." AEDC-TR-70-163 (AD872475), August 1970.

5. ICRPG Handbook for Estimating the Uncertainty in Measurements Made with Liquid Propellant Rocket Engine Systems. Interagency Chemical Rocket Propulsion Group CPIA No. 180, April 30, 1969.

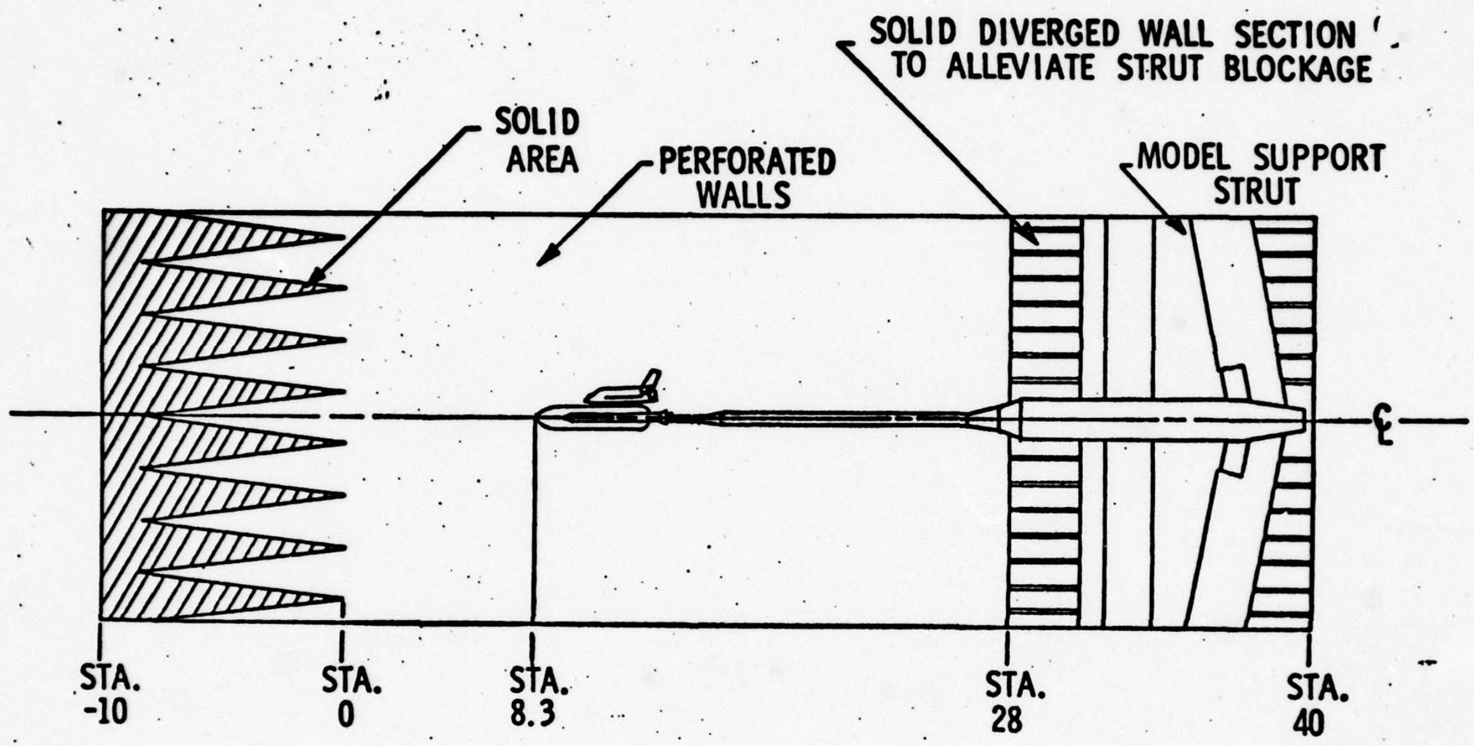

a. Sting Support System

Figure 1. Location of the Model in the 16T Test Section

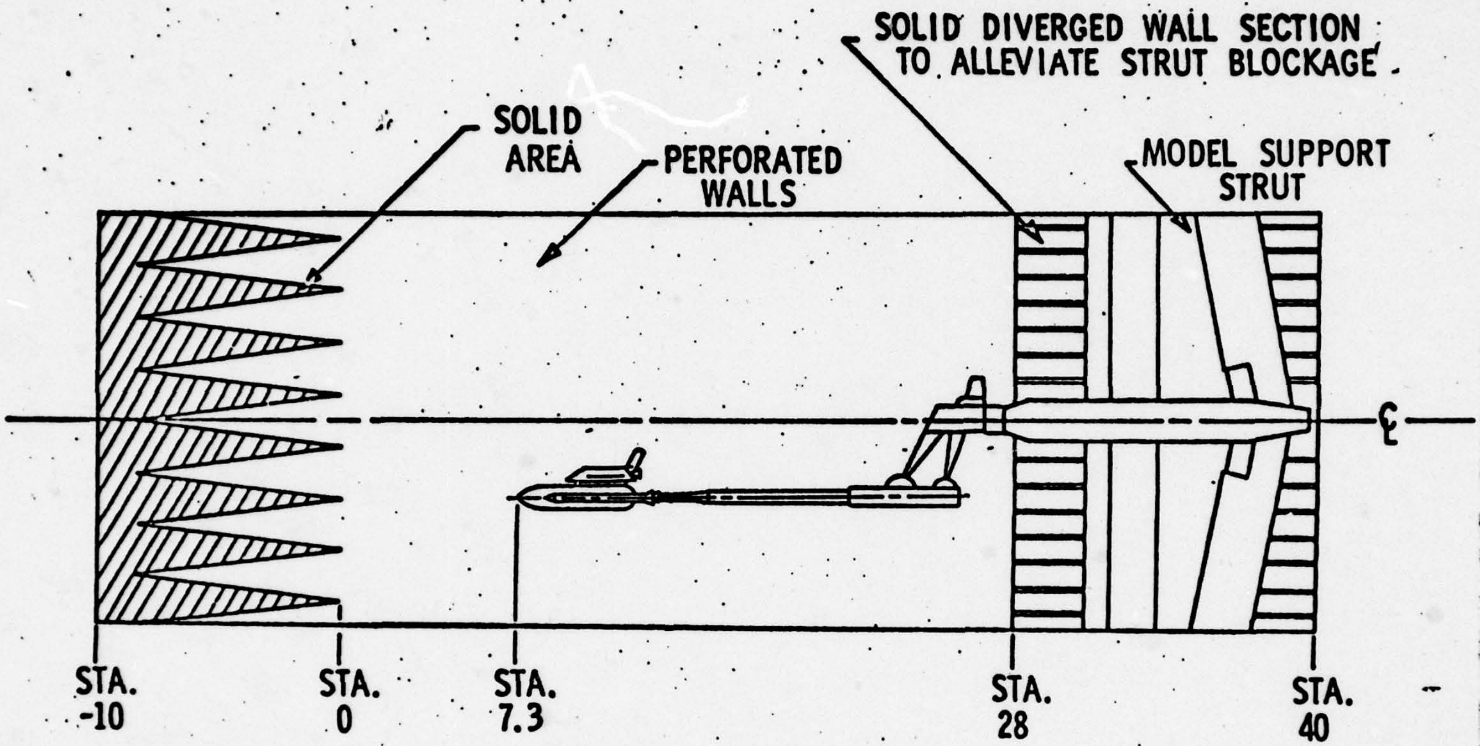

b. High Pitch Support System

Figure 1. Concluded

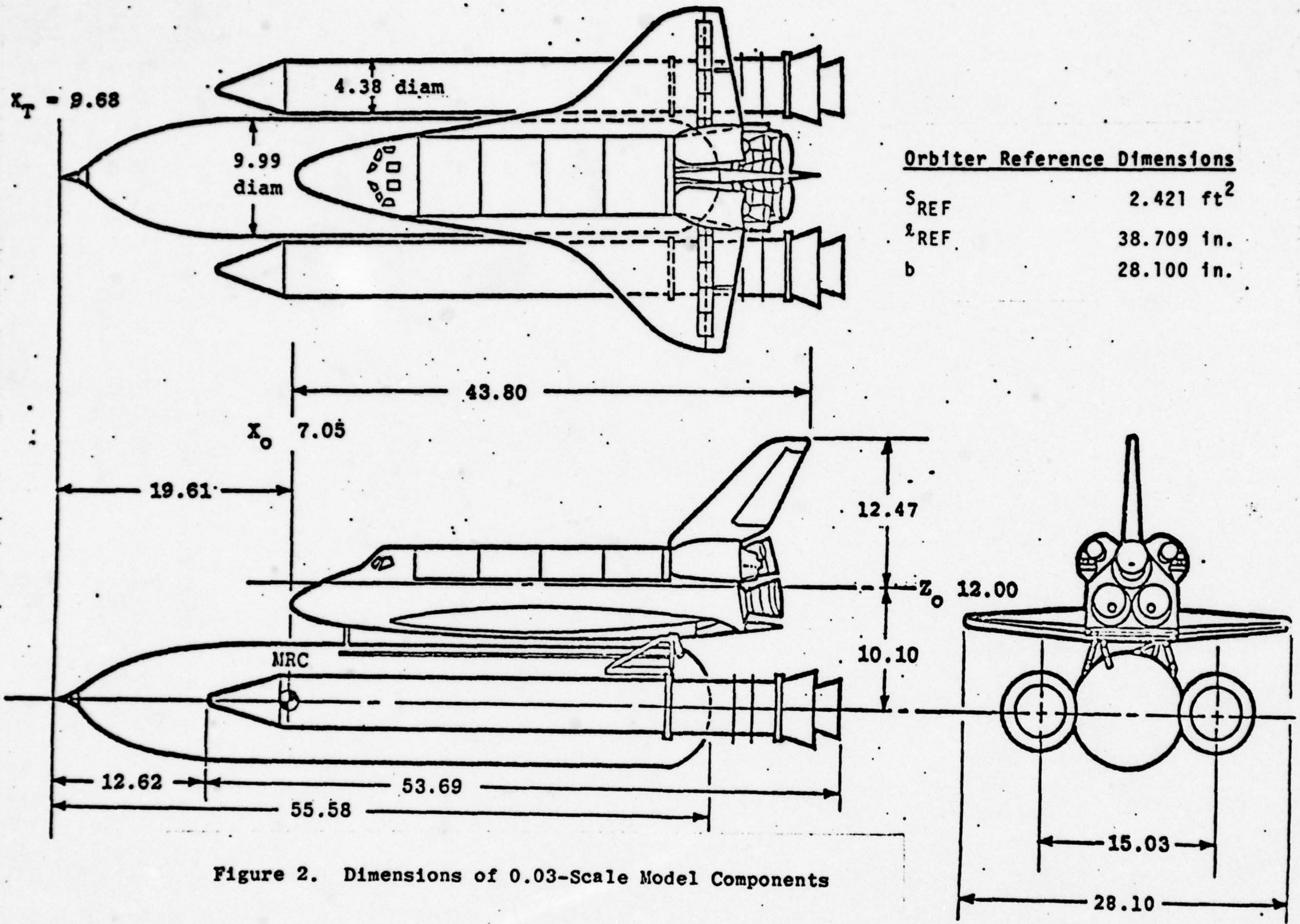

Orbiter Reference Dimensions

S_{REF}	2.421 ft^2
ℓ_{REF}	38.709 in.
b	28.100 in.

Figure 2. Dimensions of 0.03-Scale Model Components

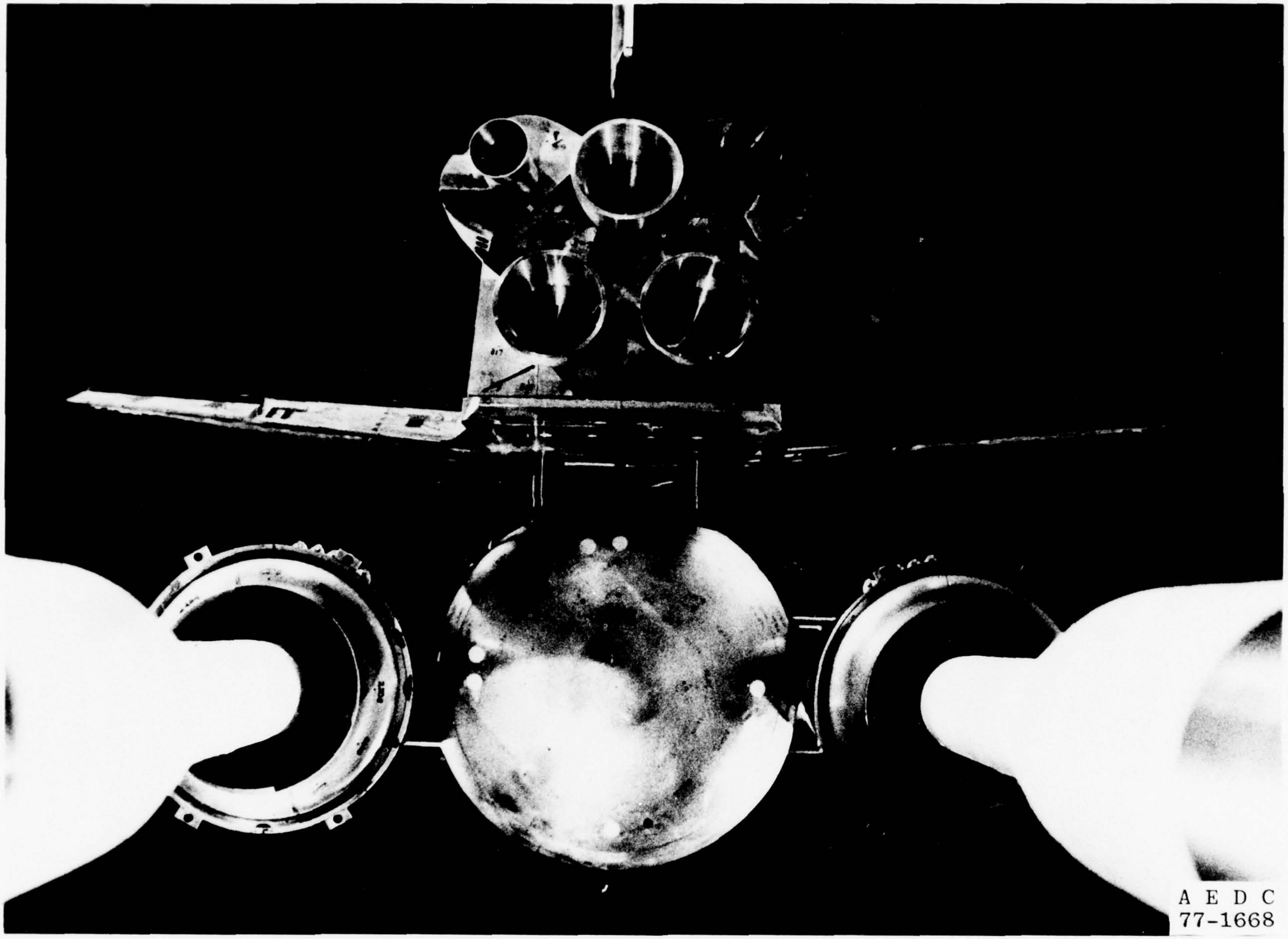

Figure 3. Launch Vehicle Base

Figure 4. Model Installation on the Sting Support System

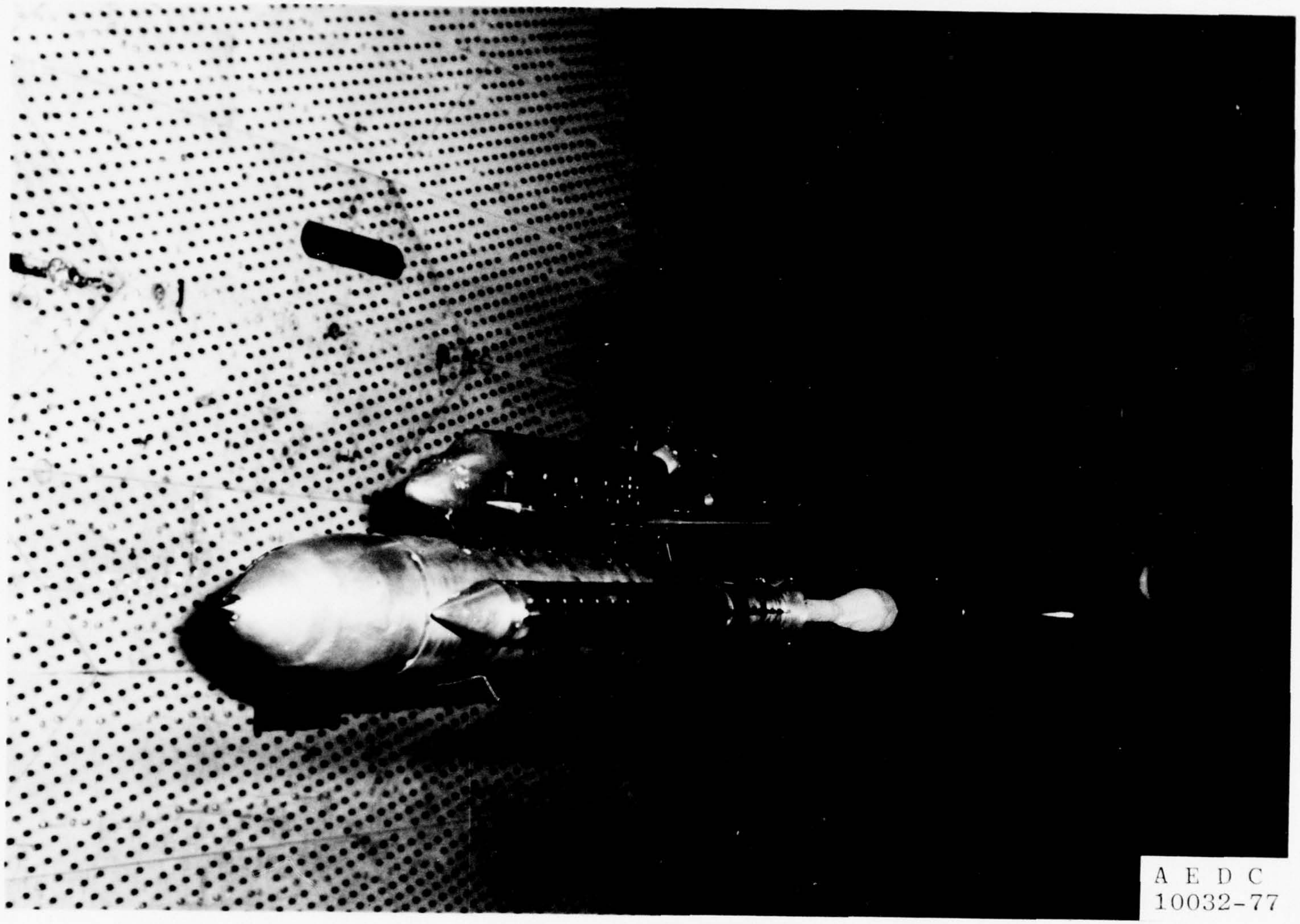

Figure 5. Model Installation on the Hi-Pitch Support System

Orifice	Zo	Yo
303	13.29	0
307	9.06	0
312	13.17	-2.34
316	11.28	-3.09
318	9.06	-3.09
319	15.42	-1.65
321	15.66	-3.09
323	13.17	-3.21
304	12.00	0

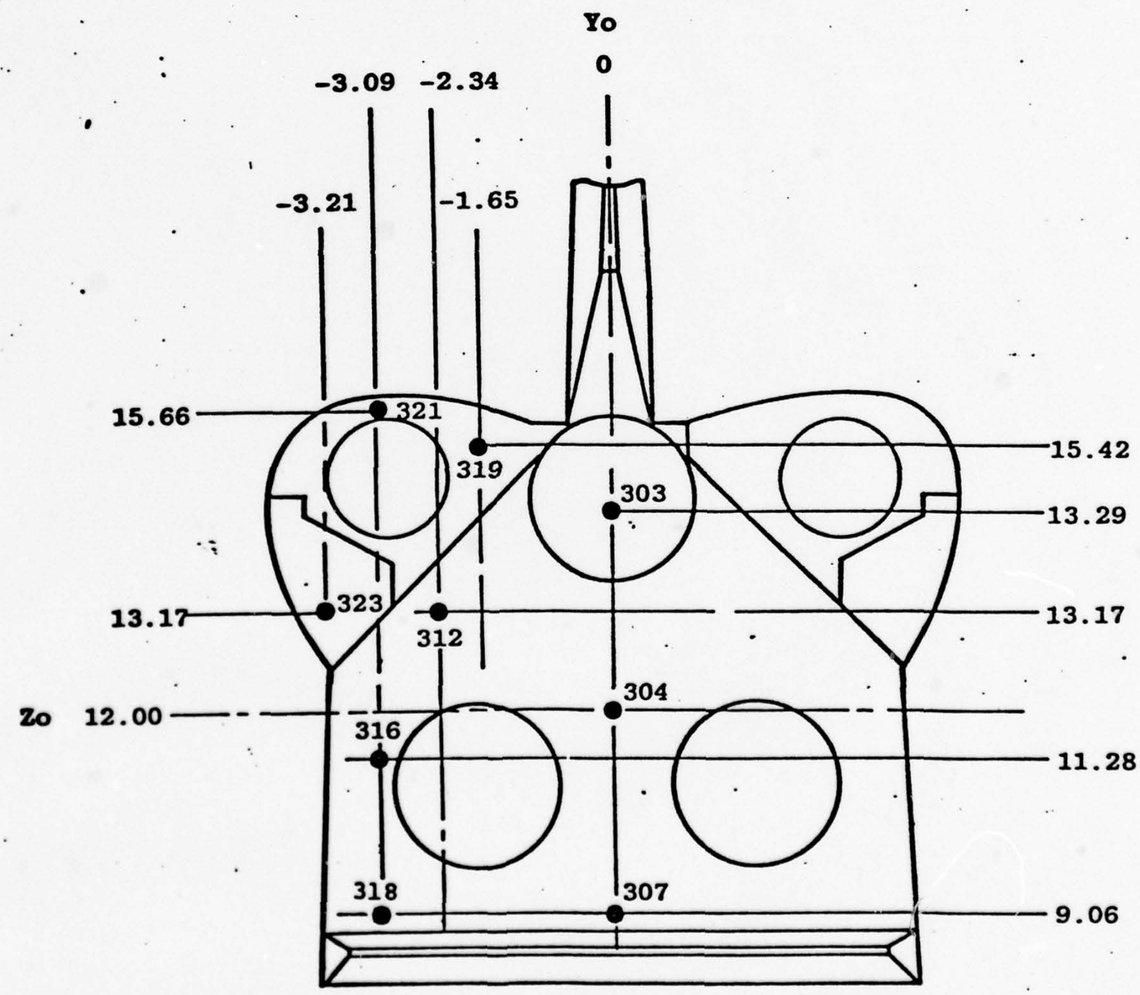

a. Orbiter Base Pressure Instrumentation

Figure 6. Pressure Orifice Locations

η	X/C_{BF} (Top)		
	-0.10	0.60	0.95
0.10	405		408
0.50	413		416
0.90	437	439	440

C_{BF} = 2.43 in.

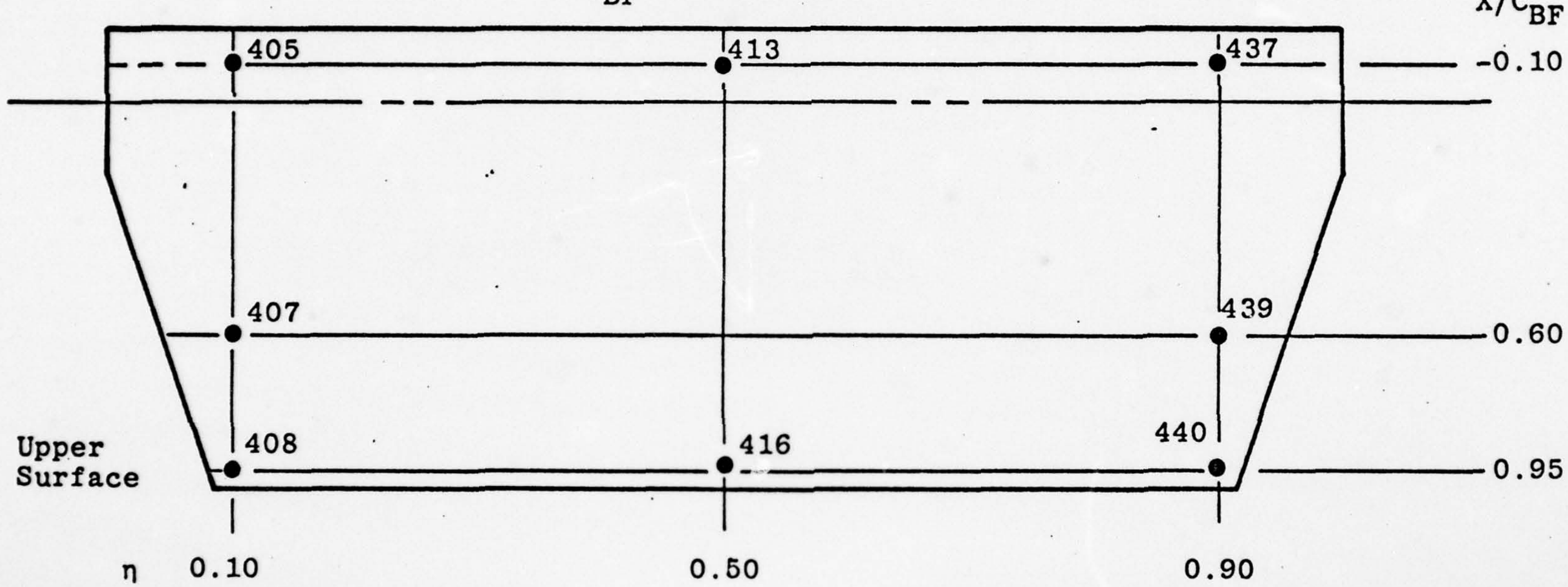

b. Orbiter Body Flap Pressure Instrumentation

Figure 6. Continued

Number	Xo	ϕo	Yo	Zo
220	39.54	135	2.6730	14.6730
225	40.50	135	3.1207	15.1206

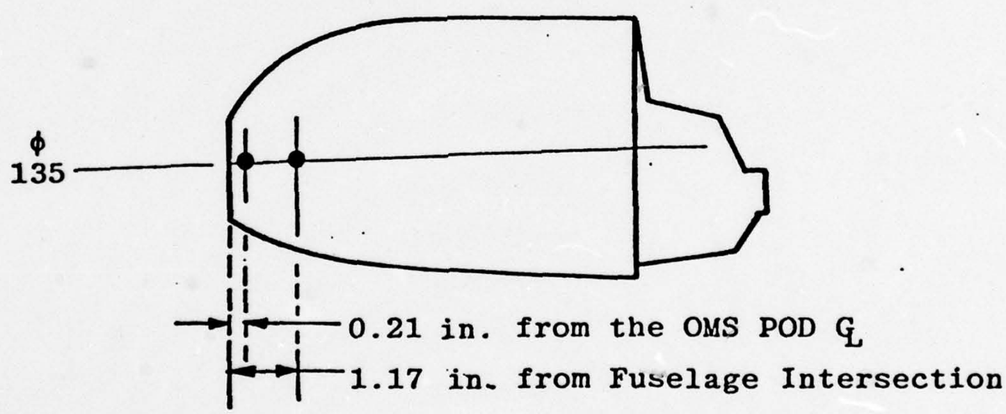

c. Orbiter OMS Pod Instrumentation

Figure 6. Concluded

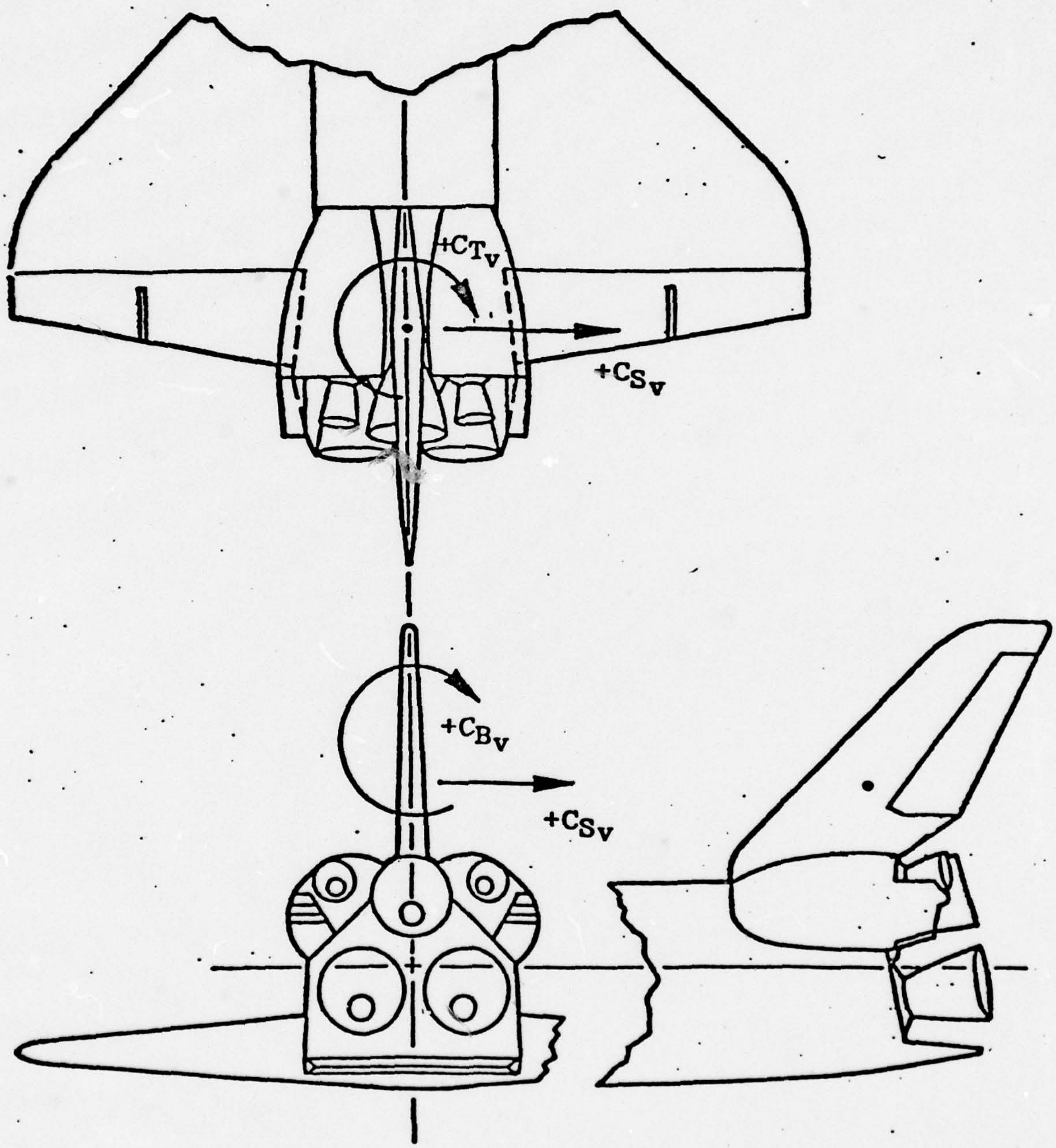

a. Vertical Stabilizer Forces and Moments

Figure 7. Force and Moment Directional Definitions and Moment Reference Locations

Vertical Stabilizer Reference Dimensions

S_{REF}	0.372 ft^2
ℓ_{REF}	5.994 in.

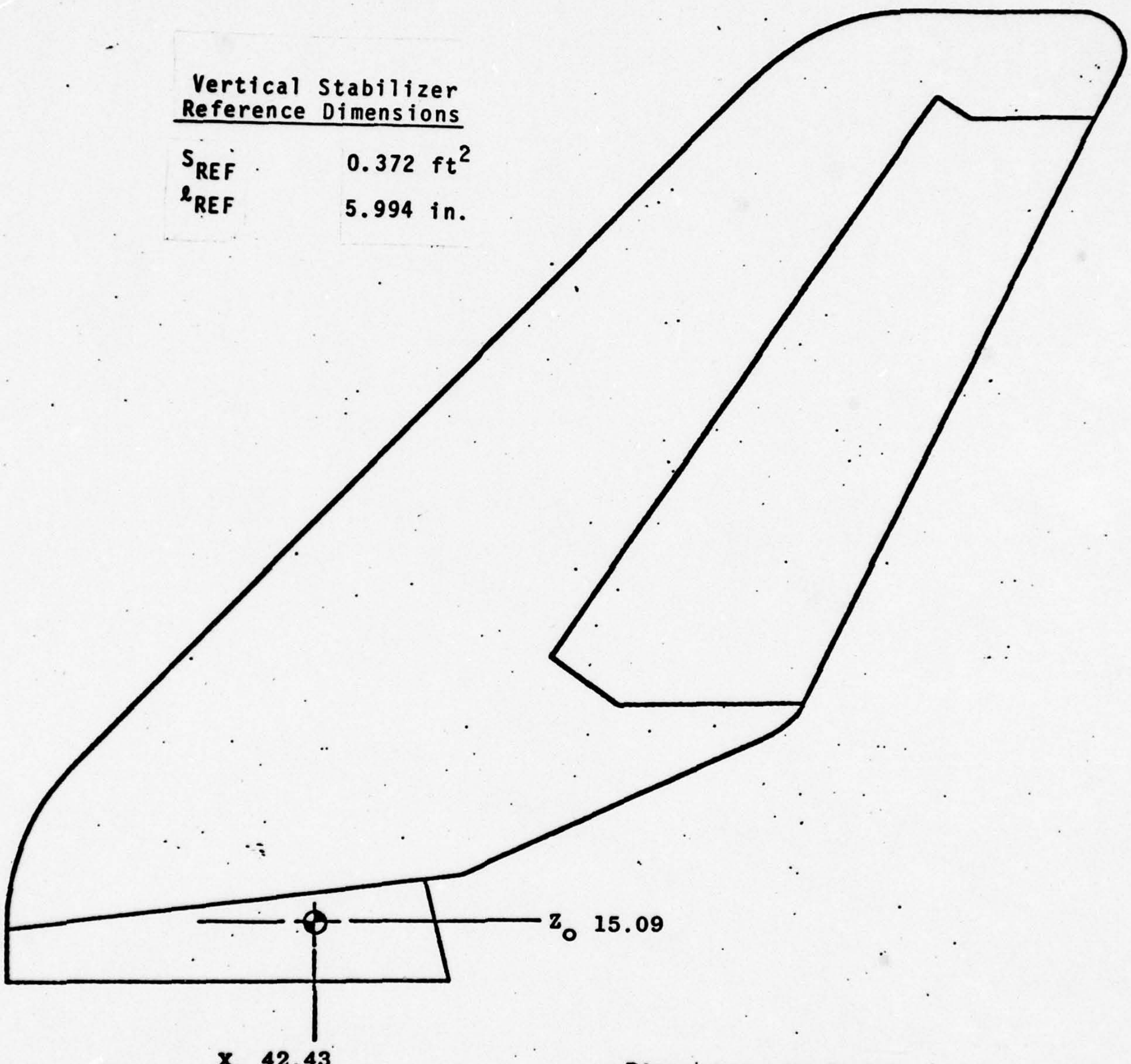

Dimensions in Inches

b. Vertical Stabilizer Moment Reference Center

Figure 7. Continued

Elevon Reference Dimensions	
S_{REF}	0.189 ft^2
ℓ_{REF}	2.721 in.

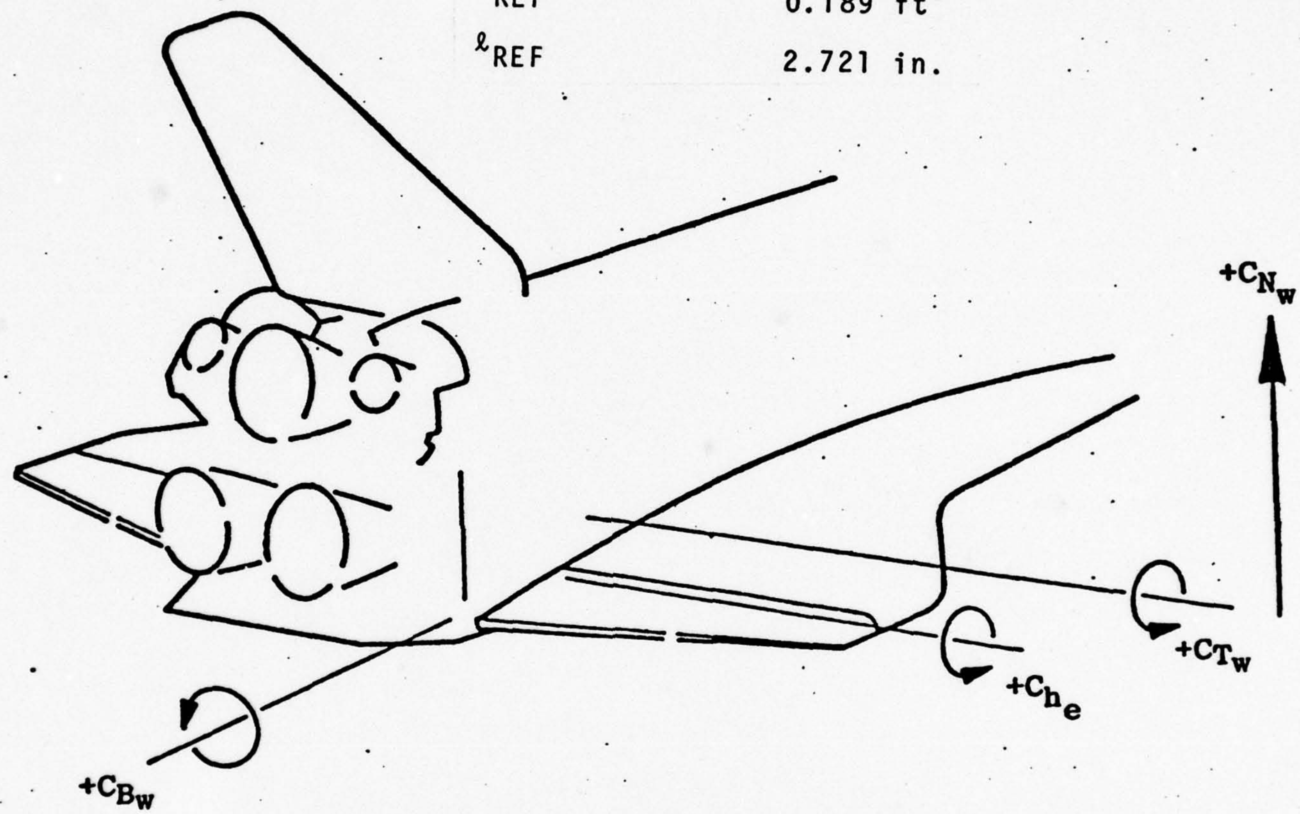

c. Wing and Elevon Forces and Moments

Figure 7. Continued

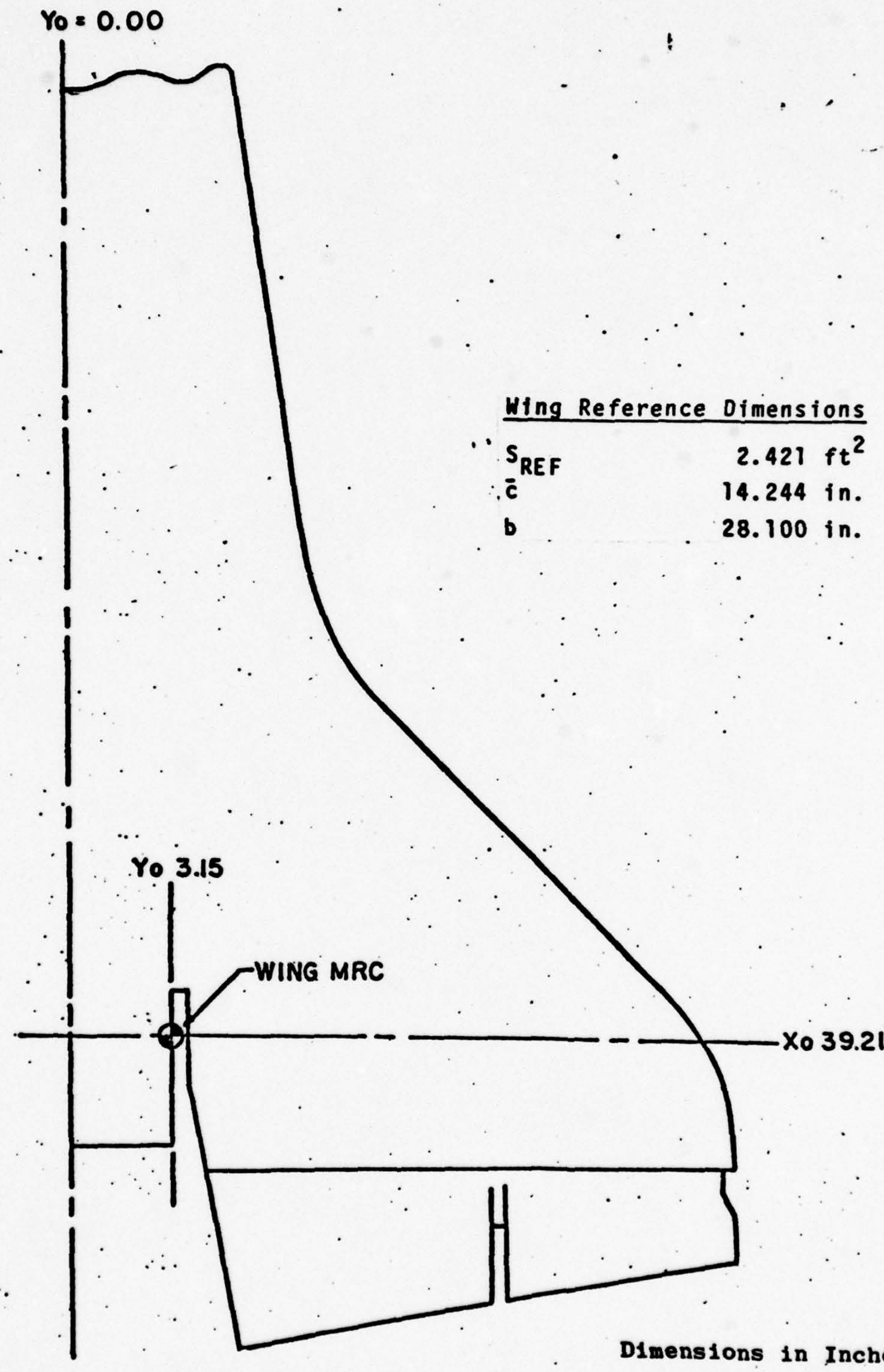

Wing Reference Dimensions

S_{REF}	2.421 ft^2
$\bar{c}$	14.244 in.
b	28.100 in.

Dimensions in Inches

d. Wing Moment Reference Center

Figure 7. Concluded

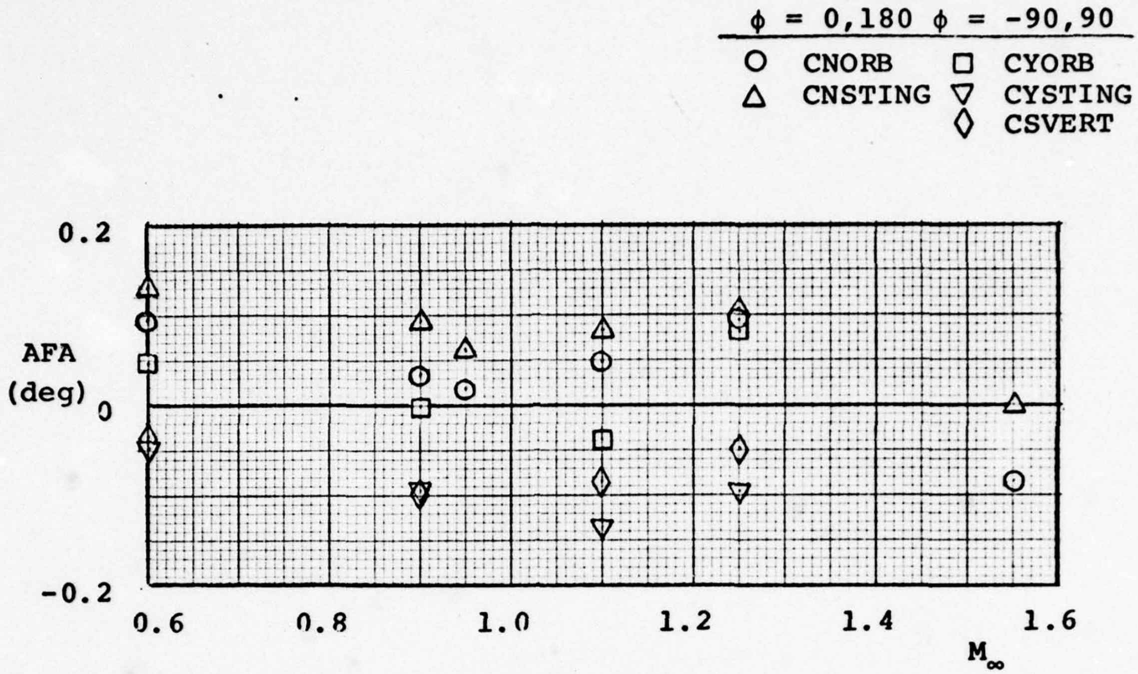

a. Pitch Plane Flow Angularity Determined from 180-deg Opposed Balance Components

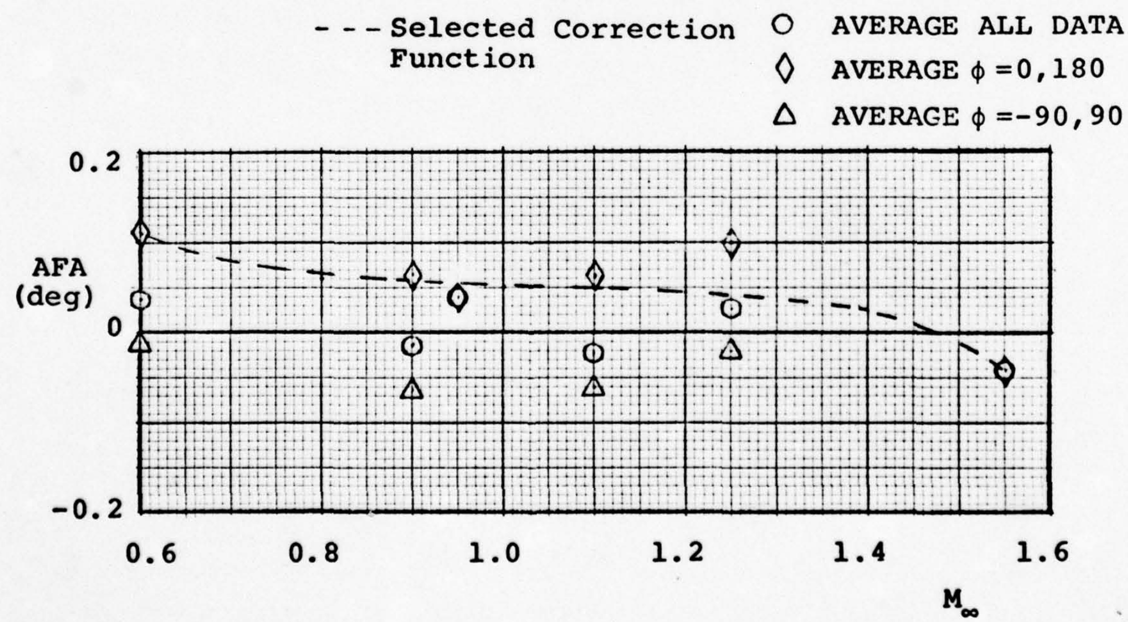

b. Averaged Values of Pitch Plane Flow Angularity

Figure 8. Pitch and Sideslip Plane Flow Angularities and Orbiter Balance Center Vertical Locations for Sting Support System Model Supported Tests

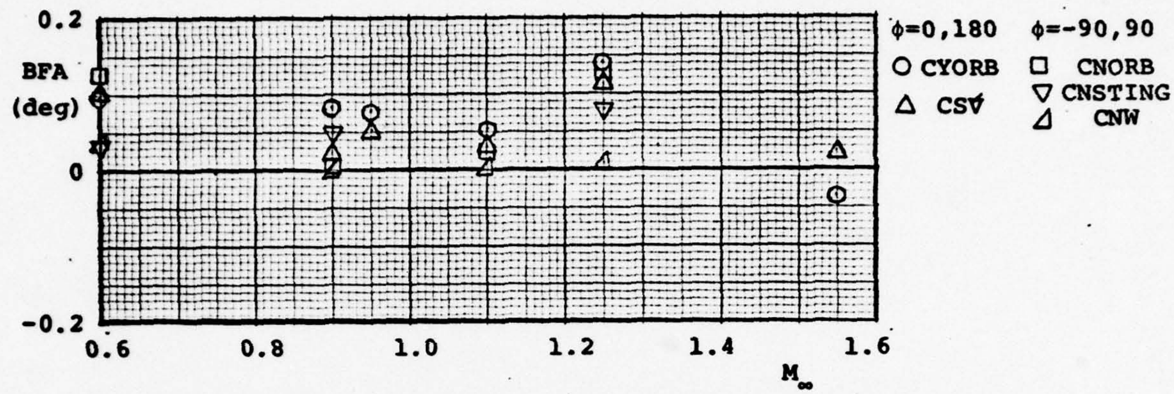

c. Sideslip Plane Flow Angularity Determined from 180-deg Opposed Balance Components

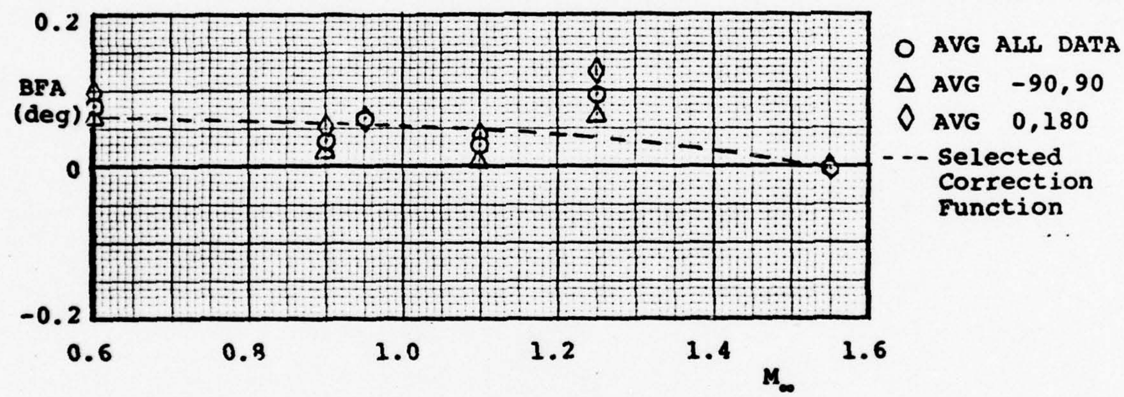

d. Averaged Values of Sideslip Plane Flow Angularity

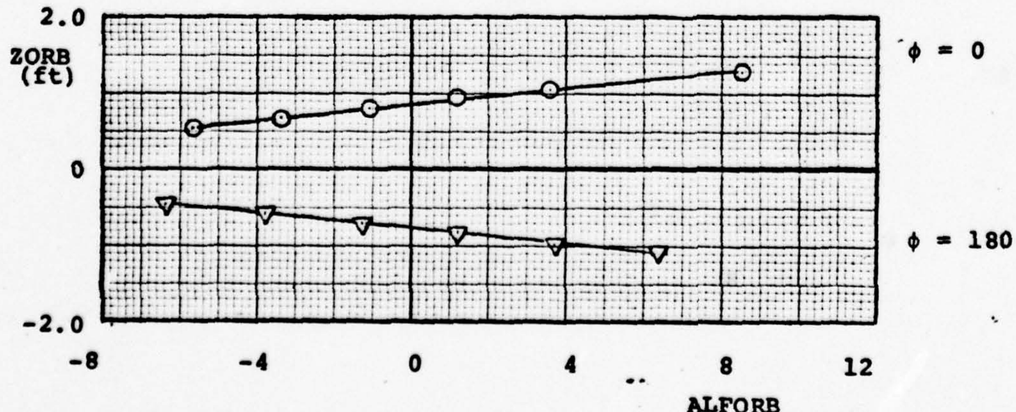

e. Variation of Orbiter Balance Center Location with Orbiter Angle of Attack

Figure 8. Concluded

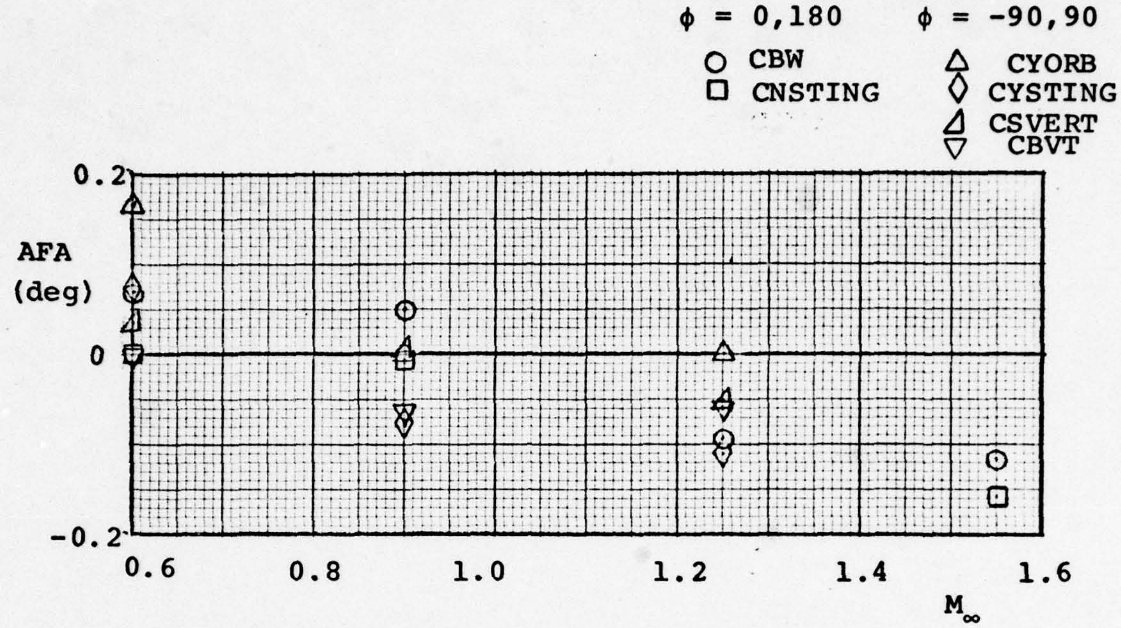

a. Pitch Plane Flow Angularity Determined from 180-deg Opposed Balance Components

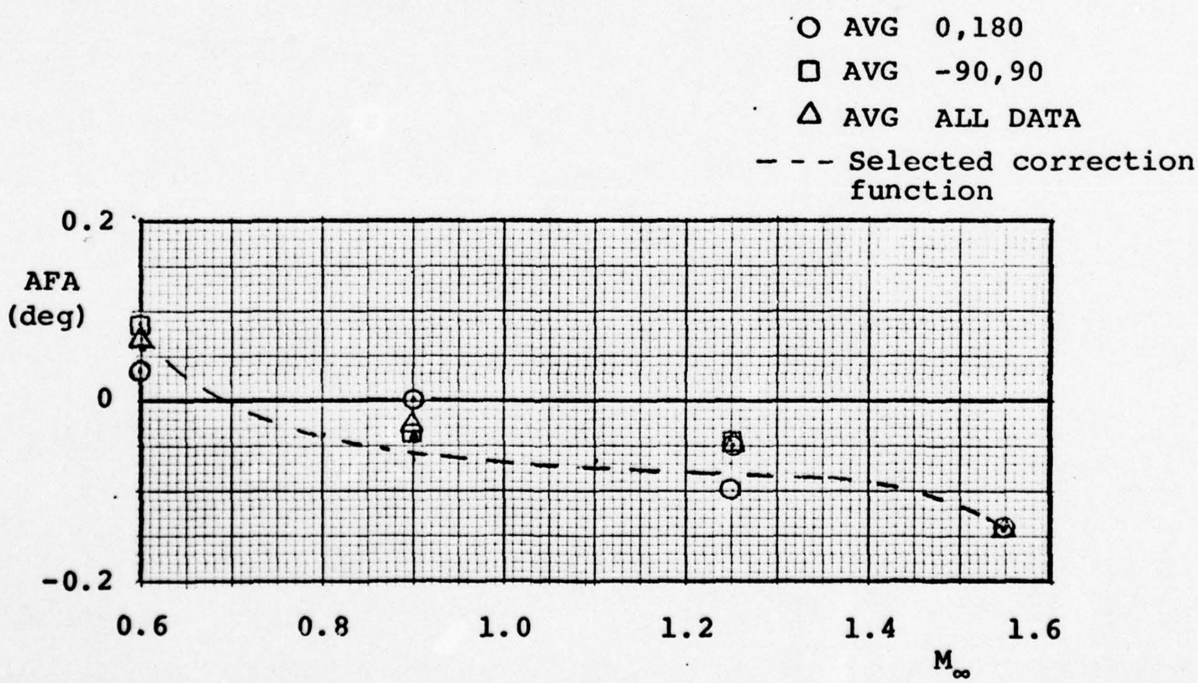

b. Averaged Values of Pitch Plane Flow Angularity

Figure 9. Pitch and Sideslip Plane Flow Angularities and Orbiter Balance Center Vertical Locations for High-Pitch Model Supported Tests

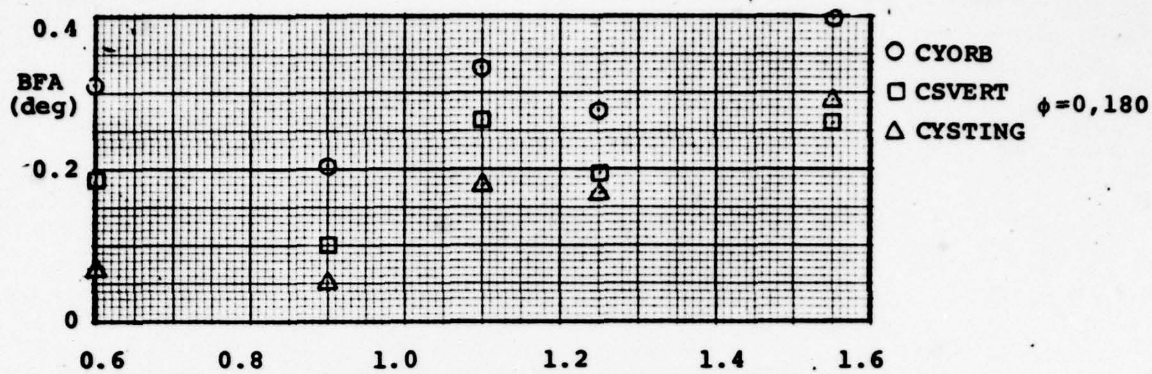

c. Sideslip Plane Flow Angularity Determined from 180-deg Opposed Balance Components

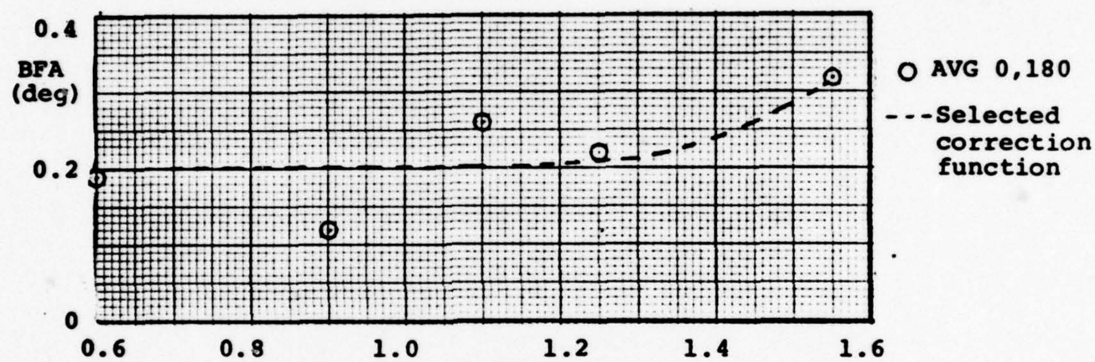

d. Averaged Values of Sideslip Plane Flow Angularity

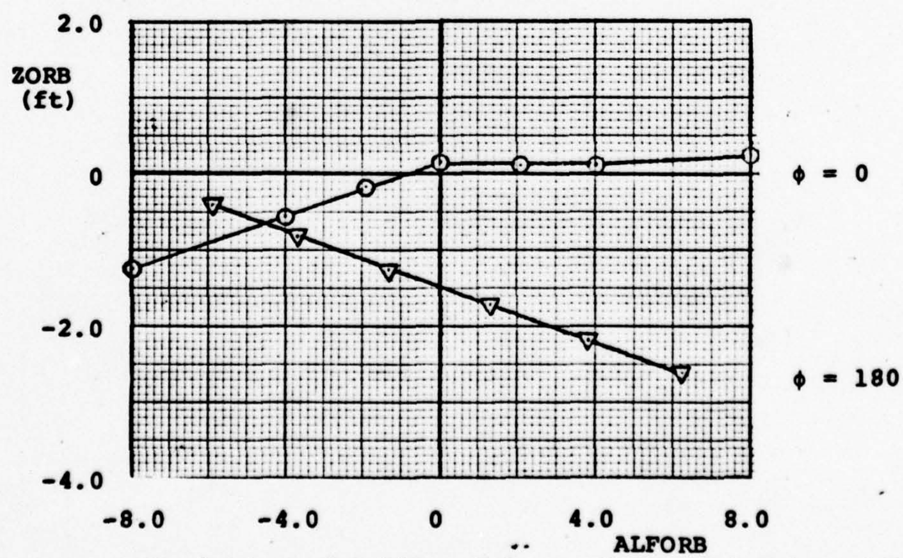

e. Variation of Orbiter Balance Center Location with Orbiter Angle of Attack

Figure 9. Concluded

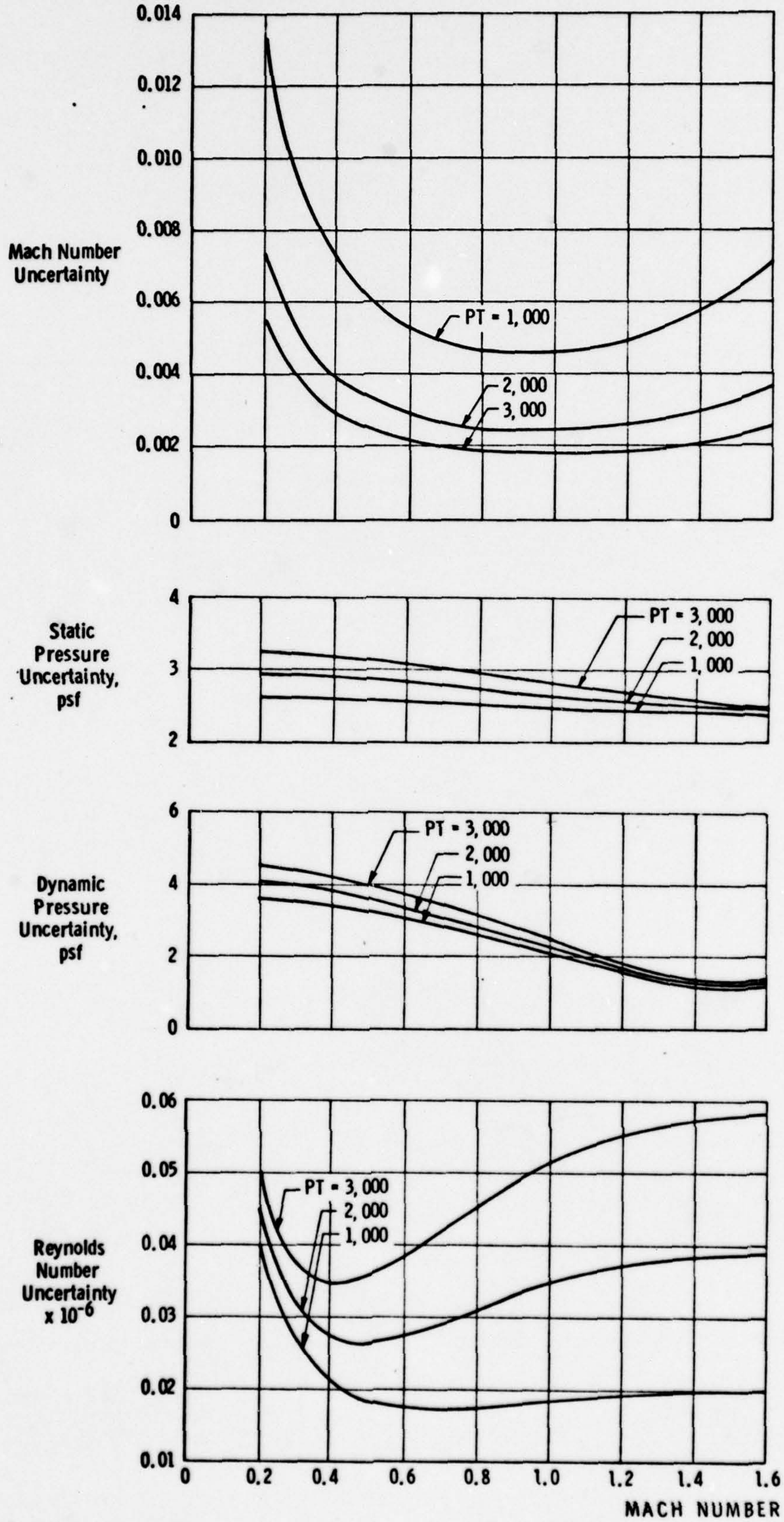

Figure 10. Estimated uncertainties in wind tunnel parameters.

Table 1.

Model Attitude Schedules and Summary of Test Conditions, First Entry

M_∞	$Re \times 10^{-6}$	α	ϕ	$\beta = 0$	Remarks
0.60	3.0	A	0	*3093	FLOW ANGULARITY INVESTIGATION
0.90		B		3094	
0.95				3097	
1.10				3098	
1.25				3099	
0.90				3101	
1.10				3102	
1.55				3103	
0.60		C	180	3106	
0.90				3107	
0.95				3108	
1.10				3109	
1.25				3110	
1.55				3111	

NOTE: * PART NUMBER

SCHEDULE	NOMINAL ANGLES
A	$\alpha = -11, -6, -4, -1, 1, 3, 8$
B	$\alpha = -8, -4, -2, 0, 2, 4, 8$
C	$\alpha = -6, -1, 1, 4, 6$
D	$\beta = -6, -4, 0, 4, 6$

M_∞	$Re \times 10^{-6}$	β	ϕ	α					Remarks
				-8	-4	0	4	8	
0.60	3.0	D	90			3115			FLOW ANGULARITY INVESTIGATION
			-90			3116			
0.90			90			3117			
			-90			3118			
1.10			-90			3119			
			90			3120			
1.25			90			3121			
			-90			3122			
1.25			VARY	3123	3124		3125		α/β MATRIX
1.55				3126	3127		3128		
			90			3129			
0.60			VARY	3132	3133		3134	3135	
0.90				3136	3137		3138		
1.10				3139	3140		3141		
1.15				3142	3143		3144		
			90			3145			
0.95						3146			
			VARY		3147				

Table 2

Model Attitude Schedules and Summary of Test Conditions, Second Entry

M_∞	Re x 10^{-6}	α	ϕ	$\beta = 0$	Remarks	
0.60	3.0	A	0	*3227		FLOW ANGULARITY INVESTIGATION
↓		B		3228	ZMAX-1	
0.90		B		3229	↓	
↓		A		3230		
0.95		A		3231		
↓		B		3232	ZMAX-1	
1.10		B		3233	↓	
↓		A		3234		
0.90		A		3237		
1.25		A		3238		
↓		B		3239	ZMAX-1	
1.55		B		3240	↓	
		A	↓	3241		
↓		C	180	3242	Z MAX	
1.25		D		3244		
1.10		D		3245	↓	
↓		E		3246	ZMAX-1	
0.90		F		3247	ZMAX	
0.60		G		3248	↓	
↓	↓	H	↓	3249	ZMAX-1	↓

M_∞	Re x 10^{-6}	β	ϕ	α				Remarks
				-8	-4	0	4	
0.60	3.0	I	90			3256		FLOW ANGULARITY INVESTIGATION
		↓	-90			3257		↓
↓		J	VARY	3258	3259		3260	α/β MATRIX
0.90		I	-90			3262		F.A.I.
		↓	90			3263		↓
↓		J	VARY	3264	3265		3266	α/β MATRIX
1.25		I	90			3267		F.A.I.
		↓	-90			3268		↓
↓	↓	J	VARY	3269	3270		3271	α/β MATRIX

NOTE : * PART NUMBER

SCHEDULE	NOMINAL ANGLES
A	$\alpha = -8, -4, -2, 0, 2, 4, 8$
B	$\alpha = -4, -2, 0, 2, 4$
C	$\alpha = -8, -4, -1, 1, 4, 7$
D	$\alpha = -7, -4, -1, 2, 4, 7$
E	$\alpha = -4, -1, 2, 4$
F	$\alpha = -7, -6, -4, -1, 1, 4, 7$
G	$\alpha = -6, -4, -1, 1, 4, 6$
H	$\alpha = -4, -1, 1, 4, 6$
I	$\beta = -6, -4, -2, 0, 2, 4, 6$
J	$\beta = -6, -4, 0, 4, 6$

Table 3

SAMPLE of DATA TABULATION

DATE. 11- 2-78 PROJECT NO. P41T-350
ARO, INC.
AEDC DIVISION
A SVERDRUP CORPORATION COMPANY
PROPULSION WIND TUNNEL
ARNOLD AIR FORCE STATION, TENNESSEE

PROPULSION WIND TUNNEL
TRANSONIC 16T

PART	POINT	PROJECT	TEST	DATE	DAY HR MIN SEC	MODE	DELP	PROC DATE	WIND-OFF	SET	
3093	7	P41T-350	TF-517	9/19/78	262122137153	7	336	11-02-78	92/	1	0

M	PT	P	Q	REX10-6	TT	TTR	H	PC	DP	WA	TPR	SHX10+3	PTI	PTE	CPR
0.600	1960.0	1536.5	387.3	3.000	109.8	569.5	8583.	1547.4	412.6	0.00	1.120	16.439	1749.4	1985.8	1.135

DELEIL	DELEOL	DELEINLR	DELEONLR	DELEIR	DELEOR
10.37	4.65	10.25	4.77	10.34	4.81

ALFORB	BETORB	PHIORB	ALFI	PHII	DALFS	ALFC	ALFSRB	BETSRB	ALFET	BETET
1.23	0.07	0.0	2.00	0.0	-0.73	1.84	1.23	0.07	1.23	0.07

RATD	ATD	AFA	BFA	DALFORB	DBETORB	DPHIORB	ALFORBU	BETORBU
0.1530	0.99	0.11	0.07	0.00	-0.00	0.03	1.12	0.00

	GAGE VOLTAGE						GAGE TOTAL LOAD					
	1	2	3	4	5	6	1	2	3	4	5	6
STNGL	0.0706	0.0524			0.2911	-0.0066	-1862.3	-6497.5			-6861.1	-6623.9
STNGR	0.0223	0.0440			0.2405	-0.0775	-5662.5	-5002.4			-8963.3	-6633.2
ORB	0.1590	0.0191	0.7792	0.0423	0.3942	-0.0365	4.7	2.0	59.9	37.4	35.8	-5.6
VERT	0.0	0.1248	-0.0009	-0.1575	-0.0013	0.2277	0.0	14.8	0.0	-10.1	0.0	11.4
WING	0.9886			0.0771	1.2044		280.0			31.6	361.9	
ELEVI	-0.1891						4.815					
ELEVO	-0.2223						1.619					

	BALANCE GROSS LOADS						STATIC TARES					
	FNG	FYG	FAG	MMG	MLG	MNG	FNST	FYST	FAST	MMST	MLST	MNST
STING	-346.7	-2.3		-5837.3		0.0	-422.22	0.07		-6565.5		0.0
ORB	40.4	-3.6	59.90	-132.8	37.4	27.8	-143.27	0.10	2.76	171.1	15.43	0.2
VERT	0.0	-1.55	0.0	0.0	-10.10	13.1	0.0	0.00	0.0	0.0	0.01	-0.01
WING	62.09			321.0	31.6		-14.62			-31.294	-16.55	
ELEVI				4.815						0.682		
ELEVO				1.619						0.169		

	BALANCE AERO LOADS AT MRC											
	FN	FY	FA	MM	ML	MN	A	B	C	ZORB	ZVT	ZTN
STING	75.5	-2.40		-2077.3		0.0		0.0002	0.9998	0.93	1.15	0.24
ORB	183.7	-3.67	57.14	-4466.2	-14.1	121.7	-0.0195	0.0007	0.9998			
VERT		-1.55			-9.11	9.77	-0.0195	0.0007	0.9998			
WING	76.71			397.6	229.14				0.9998			
ELEVI				4.133					0.9998			
ELEVO				1.450					0.9998			

Table 3 Continued

PART	POINT	PROJECT	TEST	M	PT	P	Q	RX10-6	TT
3093	7	P41T-35	TF-517	0.600	1960.0	1536.5	387.3	3.000	110.

ALFORB	BETORB	ALFORBU	BETORBU	AFA	BFA	DELEIL	DELEOL	DELEIR	DELEOR
1.23	0.07	1.12	0.00	0.11	0.07	10.37	4.65	10.34	4.81

P1901	P1902	P1010	P1012	P1014	P1016	P220	P225	P303	P319	P321	P323
1867.7	1852.9	1841.0	1827.7	1801.8	1818.2	1551.8	1422.8	1465.4	0.0	1459.9	1445.8

P304	P307	P312	P316	P318	P405	P407	P408	P413	P416	P437	P439	P440
1448.0	1449.1	1447.3	1444.8	1446.7	1449.1	1442.2	1442.0	1449.7	1445.2	1449.2	1442.2	1440.5

CPBA	CPOMSA	CPBFA	CPHOMA
-0.2307	-0.2159	-0.2362	-0.2071

PRESSURE COEFFICIENTS

CP1901	CP1902	CP1010	CP1012	CP1014	CP1016	CP220	CP225	CP303	CP319	CP321	CP323
0.8551	0.8168	0.7860	0.7518	0.6849	0.7272	0.0394	-0.2936	-0.1836	9.9999	-0.1978	-0.2341

CP304	CP307	CP312	CP316	CP318	CP405	CP407	CP408	CP413	CP416	CP437	CP439	CP440
-0.2286	-0.2258	-0.2304	-0.2369	-0.2318	-0.2256	-0.2435	-0.2441	-0.2242	-0.2358	-0.2254	-0.2434	-0.2479

ORBITER COEFFICIENTS

ALFORB	BETORB	CNF	CY	CAF	CMF	CLL	CLN	CNU	CNB	CAU	CAB	CMU	CMB
1.23	0.07	0.1770	-0.0039	0.0265	-0.1126	-0.0004	0.0034	0.1959	0.0189	0.0609	0.0344	-0.1230	-0.0105

VERTICAL TAIL COEFFICIENTS

CSVT	CHVT	CTVT	XCPV	ZCPV
-0.0108	-0.0105	0.0113	1622.81	698.40

MODEL LOCATIONS

ZORB	ZVT	ZTN	ZSTRUT
0.93	1.15	0.24	0.0

WING COEFFICIENTS

CNW	CBW	CTW
0.0818	0.0151	0.0172

ELEVON COEFFICIENTS

CHEI	CHEO
0.0207	0.0073

STING COEFFICIENTS

CN	CLM	CY
0.0805	-0.0572	-0.0026

Table 4

Data Tabulation Nomenclature

Tunnel Parameters

CPR	Compressor pressure ratio
DATE	Date of data acquisition
DAY	Day (of year) of data acquisition
DELP	Primary input deletion and selection code
DP	Differential pressure, (PT-PC), psf
H	Pressure altitude, ft
HR	Hour of data acquisition
M	Free-stream Mach number
MIN	Minute of data acquisition
MODE	Data acquisition mode
P	Free-stream static pressure, psfa
PART	Part number (a data subset containing variations of only one independent parameter
POINT	Point number (a single record of all test parameters)
PROC DATE	Date of data processing
PROJECT	AEDC project number
PT	Free-stream total pressure, psfa
PTE	Compressor exit pressure, psfa
PTI	Compressor inlet pressure, psfa
Q	Free-stream dynamic pressure, psf
Rex10-6	Free-stream unit Reynolds number, per foot
SEC	Second of data acquisition
SET	Constant set used

Table 4. Continued

SHX10+3	Tunnel specific humidity, lb/lb
TEST	AEDC test number
TPR	Tunnel pressure ratio
TT	Free-stream stagnation temperature, °F
TTR	Free-stream stagnation temperature, °R
WA	Test section wall angle, deg
WINDOFF	Wind-off part and point number

Test Parameters

A	Trigonometric function used in determining model static tares
AFA	Flow angularity in the tunnel pitch plane, positive up, deg
ALFC	Effective sting pitch angle, deg
ALFET	External tank angle of attack, deg
ALFI	Sting pitch angle, deg
ALFORB	Orbiter angle of attack, deg
ALFORBU	Orbiter angle of attack uncorrected for flow angularity, deg
ALFSRB	Solid rocket booster angle of attack, deg
ATD	ET angle of attack as measured by a strain gage pendulum, deg
B	Trigonometric function used in determining model static tares
BETET	External tank sideslip angle, deg
BETORB	Orbiter sideslip angle, deg
BETORBU	Orbiter sideslip angle uncorrected for flow angularity, deg
BETSRB	Solid rocket booster sideslip angle, deg

Table 4. Continued

BFA	Flow angularity in the tunnel cross flow plane, positive from right to left looking upstream, deg
C	Trigonometric function used in determining model static tares
CPBA	Average of base pressure coefficients
CPBFA	Average of body flap pressure coefficients
CPBOMA	$CPBOMA = \frac{CPBA + CPMPS}{2}$, where CPMPS is defined as the main propulsion system pressure coefficients
CPOMSA	Average of orbiter maneuvering system (OMS) pressure coefficients
DALFORB	Orbiter deflection in the pitch plane relative to the external tank, deg
DALFS	Deflection of the sting support system in the pitch plane, deg
DBETORB	Orbiter deflection in the sideslip plane relative to the external tank, deg
DELEIL	Left hand inboard elevon nominal deflection angle, deg
DELEINLR	Right hand inboard elevon deflection angle in an unloaded condition, deg
DELEIR	Right hand inboard elevon deflection angle including deflections resulting from aero loading, deg
DELEOL	Left hand outboard elevon nominal deflection angle, deg
DELEONLR	Right hand outboard elevon deflection angle in an unloaded condition, deg
DELEOR	Right hand outboard elevon nominal deflection angle, deg
DPHIORB	Orbiter deflection rotation angle relative to the external tank, deg
FA	Model aerodynamic axial force, lb
FAG	Total axial force on balance (including static tare force), lb

Table 4. Continued

FAST	Axial force static tare, lb
FN	Model aerodynamic normal force, lb
FNG	Total normal force on balance (including static tare force), lb
FNST	Normal force static tare, lb
FY	Model aerodynamic side force, lb
FYG	Total side force on balance (including static tare force), lb
FYST	Side force static tare, lb
GAGE TOTAL LOAD	Balance gage total loads, lb
GAGE VOLTAGE	Balance gage total loads, volts
ML	Model aerodynamic rolling moment about the model reference point, in.-lb
MLG	Total rolling moment measured by balance (including static tare loads), in.-lb
MLST	Rolling moment static tare, in.-lb
MM	Model aerodynamic pitching moment about the model reference point, in.-lb
MMG	Total pitching moment measured by balance (including static tare loads), in.-lb
MMST	Pitching moment static tare, in.-lb
MN	Model aerodynamic yawing moment about the model reference point, in.-lb
MNG	Total yawing moment measured by balance (including static tare loads), in.-lb
MNST	Yawing moment static tare, in.-lb
ORB	Orbiter
PHII	Sting rotation angle, deg

Table 4. Continued

PHIORB	Orbiter angle of rotation, deg
P_n	Model pressure, psfa
RATD	Voltage output from strain gage pendulum in ET
STING	(STINGL + STINGR)/2
STINGL	Left hand sting 4-component balance
STINGR	Right hand sting 4-component balance
VERT	Vertical tail balance
WING	Wing balance
ZORB	Location of orbiter moment reference center relative to the tunnel centerline, positive above, ft
ZVT	Location of a reference point on the vertical tail surface relative to the tunnel centerline, positive above, ft
1-6	Individual balance gage loadings, lb, in.-lb, or volts

Pressure Coefficients

CP_n	Model pressure coefficients, $\frac{P_n - P_\infty}{Q}$

Orbiter Coefficients

CAB	Base axial force coefficient, body axes, force/QS_{REF}
CAF	Forebody axial force coefficient, body axes, CAF = CAU - CAB
CAU	Measured axial force coefficient, body axes, force/QS_{REF}
CLL	Orbiter rolling moment coefficient, body axes, moment/$Q(S_{REF})b$
CLN	Orbiter yawing moment coefficient, body axes, moment/$Q(S_{REF})b$

Table 4. Continued

CMB	Base pitching-moment coefficient, moment/$Q(S_{REF})\ell_{REF}$
CMF	Forebody pitching-moment coefficient, CMU - CMB
CMU	Uncorrected pitching-moment coefficient, moment/$Q(S_{REF})\ell_{REF}$
CNB	Base normal force coefficient, force/QS_{REF}
CNF	Forebody normal force coefficient, CNU - CNB
CNU	Measured normal force coefficient, force/QS_{REF}
CY	Orbiter side force coefficient, force/QS_{REF}

<u>Vertical Tail Coefficients</u>

CBVT	Vertical tail bending moment coefficient, moment/$Q(S_{VT})(C_{VT})$
CSVT	Side force coefficient of the vertical tail, force/QS_{VT}
CTVT	Torsional moment coefficient of the vertical tail, moment/$Q(S_{REF})(\ell_{REF})$
XCPV	Longitudinal center-of-pressure location in full scale coordinates, in.
ZCPV	Vertical center-of-pressure location in full scale coordinates, in.

<u>Wing Coefficients</u>

CBW	Bending moment coefficient of the wing, moment/$Q(S_{REF})b$
CNW	Normal force coefficient of the wing, force/QS_{REF}
CTW	Torsional moment coefficient of the wing, moment/$Q(S_{REF})\bar{c}$

Table 4. Concluded

Elevon Coefficients

CHEI	Inboard elevon hinge moment coefficient, moment/$Q(S_{REF})(\ell_{REF})$
CHEO	Outboard elevon hinge moment coefficient, moment/$Q(S_{REF})(\ell_{REF})$

Sting Coefficients

CLM	Pitching-moment coefficient of the sting, moment/$Q(S_{REF})L_{REF}$
CN	Normal force coefficient of the sting, force/$Q(S_{REF})$
CY	Side force coefficient of the sting, force/$Q(S_{REF})$

APPENDIX

UNCERTAINTY OF FLOW ANGULARITY MEASUREMENTS

R. E. Graham
Analysis and Evaluation Division (DOTA)
Arnold Engineering Development Center

An analysis of the overall uncertainty of the flow angle measurements has been made based upon selected results from the test. Those results selected as representative (see text for rationale) are presented in Table A-1 and were used in the present study.

A backward elimination regression analysis was done for the sting and high-pitch support systems AFA and BFA results using a cubic polynomial in M as the trial mathematical model. By this process, those terms of powers of M determined significant by the F test at the 95% confidence level were retained in the regression equation. It was determined that the sting support AFA and BFA were best represented as a cubic polynomial in M, that the high pitch AFA was linear with M and that the high pitch BFA was independent of M. The standard errors of estimate $\hat{S}$ (at the mean) resulting are given in Table A-2.

It was determined by using the F statistic (formed from the ratio of variances) that at the 95% confidence level, the $\hat{S}$'s of the sting AFA, sting BFA and high-pitch AFA could be pooled to form a combined standard error $\hat{S}_{pooled} = 0.048$ deg with a degrees of freedom $\nu_{pooled} = 48$. The pooled $\hat{S}$ and the high-pitch BFA were then combined using the root sum squared relationship yielding $\hat{S}_{combined} = 0.128$ deg with a combined degrees of freedom $\nu_{combined} = 12$ (from the Welch-Satterthwaite formula). The uncertainty of the flow angularity measurements at the 95% confidence level for the combined results $U_{95\%}$ was determined by the following relationship where $t_{\alpha/2}, \nu_{combined}$ represents the Student's t value at 0.025 and ν of 12

$$U_{95\%} = \pm(t_{\alpha/2}, \nu_{combined}) * \hat{S}_{combined}$$

$$U_{95\%} = \pm 0.279 \text{ deg.}$$

Table A-1

Flow Angularities (deg) as a Function of Mach Number and Coefficient

Sting Support System

M_∞	AFA	Coeff. Code
0.60	0.095	1
0.90	0.036	1
0.95	0.020	1
1.10	0.048	1
1.25	0.095	1
1.55	-0.083	1
0.60	0.131	2
0.90	0.095	2
0.95	0.060	2
1.10	0.083	2
1.25	0.107	2
1.55	0.000	2
0.60	0.048	3
0.90	0.000	3
1.10	-0.036	3
1.25	0.083	3

M_∞	BFA	Coeff. Code
0.60	0.098	4
0.90	0.086	4
0.95	0.079	4
1.10	0.054	4
1.25	0.144	4
1.55	-0.032	4
0.60	0.107	5
0.90	0.023	5
0.95	0.053	5
1.10	0.032	5
1.25	0.112	5
1.55	0.025	5
0.60	0.127	10
0.90	0.007	10
1.10	0.024	10
1.25	0.130	10
0.60	0.034	11
0.90	0.050	11
1.25	0.079	11
0.60	0.034	12
0.90	0.000	12
1.10	0.000	12
1.25	0.010	12

Coefficient Code	Source
1	CNORB, ϕ = 0,180
2	CNSTING, ϕ = 0,180
3	CYORB, ϕ = -90,90
4	CYORB, ϕ = 0,180
5	CSVT, ϕ = 0,180
10	CNORB, ϕ = -90,90
11	CNSTING, ϕ = -90,90
12	CNWING, ϕ = -90,90

Table A-1. Concluded

High-Pitch Support System

M_∞	AFA	Coeff. Code
0.60	0.000	2
0.90	-0.050	2
1.55	-0.160	2
0.60	0.070	6
0.90	0.050	6
1.25	-0.100	6
1.55	-0.120	6
0.60	0.170	3
0.90	0.000	3
1.25	0.000	3
0.60	0.110	7
0.90	0.000	7
1.25	0.000	7
0.60	0.070	13
0.90	-0.080	13
1.25	-0.110	13
0.60	0.000	9
0.90	-0.070	9
1.25	-0.060	9

M_∞	BFA	Coeff. Code
0.60	0.31	4
0.90	0.20	4
1.10	0.34	4
1.25	0.28	4
1.55	0.42	4
0.60	0.07	8
0.90	0.05	8
1.10	0.18	8
1.25	0.17	8
1.55	0.29	8

Coefficient Code	Source
2	CNSTING, ϕ =0,180
3	CYORB, ϕ = -90,90
4	CYORB, ϕ = 0,180
6	CBW, ϕ = 0,180
7	CYSTING, ϕ = -90,90
8	CYSTING, ϕ = 0,180
9	CBVT, ϕ = -90,90
13	CSVT, ϕ = -90,90

Table A-2

Regression Results

Support System	Angle	Mean Angle (deg)	Standard Angle of Estimate $\hat{S}$ (deg)	No. of Samples n	Degrees of Freedom ν
Sting	AFA	0.049	0.045	16	12
Sting	BFA	0.055	0.043	23	19
High Pitch	AFA	-0.015	0.055	19	17
High Pitch	BFA	0.231	0.118	10	9